Influences of Cations and Anions in Aqueous Electrolyte on the Electrochemical Reduction of CO_2 over Cu-based Electrode

Miss Siraphat Somchit

จุฬาลงกรณ์มหาวิทยาลัย
CHULALONGKORN UNIVERSITY

A Thesis Submitted in Partial Fulfillment of the Requirements

for the Degree of Master of Engineering in Chemical Engineering

Department of Chemical Engineering

FACULTY OF ENGINEERING

Chulalongkorn University

Academic Year 2019

ผลของไอออนบวกและไอออนลบในอิเล็กโทรไลต์ต่อปฏิกิริยาการรีดักชันทางเคมีไฟฟ้าของแก๊ส
คาร์บอนไดออกไซด์บนอิเล็กโทรดฐานทองแดง

น.ส.สิรภัทร สมจิตต์

จุฬาลงกรณ์มหาวิทยาลัย
CHULALONGKORN UNIVERSITY

วิทยานิพนธ์นี้เป็นส่วนหนึ่งของการศึกษาตามหลักสูตรปริญญาวิศวกรรมศาสตรมหาบัณฑิต
สาขาวิชาวิศวกรรมเคมี ภาควิชาวิศวกรรมเคมี
คณะวิศวกรรมศาสตร์ จุฬาลงกรณ์มหาวิทยาลัย
ปีการศึกษา 2562

Thesis Title	Influences of Cations and Anions in Aqueous Electrolyte on the Electrochemical Reduction of CO_2 over Cu-based Electrode
By	Miss Siraphat Somchit
Field of Study	Chemical Engineering
Thesis Advisor	Professor JOONGJAI PANPRANOT, Ph.D.
Thesis Co Advisor	Duangamol Tungasmita, Ph.D.

Accepted by the FACULTY OF ENGINEERING, Chulalongkorn University in Partial Fulfillment of the Requirement for the Master of Engineering

.... Dean of the FACULTY OF ENGINEERING

(Professor SUPOT TEACHAVORASINSKUN, D.Eng.)

THESIS COMMITTEE

.... Chairman

(CHALIDA KLAYSOM, Ph.D.)

.... Thesis Advisor

(Professor JOONGJAI PANPRANOT, Ph.D.)

.... Thesis Co-Advisor

(Duangamol Tungasmita, Ph.D.)

.... Examiner

(Chutimon Satirapipathkul, Ph.D.)

.... External Examiner

(Assistant Professor Okorn Mekasuwandumrong, Ph.D.)

สิรภัทร สมจิตต์ : ผลของไอออนบวกและไอออนลบในอิเล็กโทรไลต์ต่อปฏิกิริยาการรีดักชันทางเคมีไฟฟ้าของแก๊สคาร์บอนไดออกไซด์บนอิเล็กโทรดฐานทองแดง. (Influences of Cations and Anions in Aqueous Electrolyte on the Electrochemical Reduction of CO_2 over Cu-based Electrode) อ.ที่ปรึกษาหลัก : ศ. ดร.จูงใจ ปั้นประณต, อ.ที่ปรึกษาร่วม : ดร.ดวงกมล ตุงคะสมิต

ในงานวิจัยนี้ศึกษาผลของอิเล็กโทรไลต์ โดยประกอบด้วย โซเดียมซัลเฟต, โซเดียมคลอไรด์, โซเดียมไฮโดรเจนคาร์บอเนต, โพแทสเซียมซัลเฟต, โพแทสเซียมคลอไรด์, โพแทสเซียมไฮโดรเจนคาร์บอเนต, ซีเซียมซัลเฟต, ซีเซียมคลอไรด์ และซีเซียมไฮโดรเจนคาร์บอเนต โดยใช้โลหะทองแดงเป็นอิเล็กโทรด และดำเนินงานในเครื่องปฏิกรณ์แบบ H-cell ที่อุณหภูมิห้องและความดันบรรยากาศ โดยวิเคราะห์ผลของไอออนบวกและไอออนลบในอิเล็กโทรไลต์ต่ออัตราการเกิดสารผลิตภัณฑ์ด้วยเครื่องแก๊สโครมาโตกราฟและนิวเคลียร์แมกเนติกเรโซแนนซ์สเปกโทรสโคป จากผลการทดลอง พบว่า อิเล็กโทรไลต์ที่ประกอบด้วยคลอไรด์ไอออน ไม่เพียงแต่ช่วยสนับสนุนการรีดักชันของแก๊สคาร์บอนไดออกไซด์แต่ยังช่วยยับยั้งปฏิกิริยาการเกิดแก๊สไฮโดรเจนซึ่งเป็นปฏิกิริยาแข่งขัน อัตราการเกิดของแก๊สคาร์บอนมอนออกไซด์ต่อแก๊สไฮโดรเจนเพิ่มขึ้น เมื่อขนาดของไอออนบวกเพิ่มขึ้น นอกจากนี้ยังศึกษาอิเล็กโทรไลต์ผสมระหว่างไฮโดรเจนคาร์บอเนตและคลอไรด์ที่ความเข้มข้นของคลอไรด์ต่างกัน พบว่าอิเล็กโทรไลต์ผสมช่วยเพิ่มประสิทธิภาพในการรีดิวซ์แก๊สคาร์บอนไดออกไซด์ และเมื่อความเข้มข้นของคลอไรด์เพิ่มขึ้นถึง 0.4 โมลาร์ อาจส่งผลให้เกิดฟิล์มของทองแดงและคลอไรด์ซึ่งช่วยส่งเสริมการแลกเปลี่ยนอิเล็กตรอนและการแพร่ของสารมัธยันตร์ ส่งผลให้เกิดสารผลิตภัณฑ์ C2 และศึกษาผลของค่าศักย์ไฟฟ้าที่ใช้ในการดำเนินงานต่อการรีดักชันของแก๊สคาร์บอนไดออกไซด์ ตั้งแต่ -1.2 ถึง -2.0 โวลต์ พบว่า การเพิ่มค่าศักย์ไฟฟ้าทำให้สารมัธยันตร์สามารถรีดิวซ์ต่อไปจนเกิดสารประกอบ C2 ได้ ประสิทธิภาพของอิเล็กโทรไลต์มีความสัมพันธ์กับค่ากระแสการรีดักชันและความต้านทานการถ่ายโอนประจุ ดังแสดงด้วยผลการทดลองจากลิเนียร์สวีปโวลาทิเมตทรีและอิเล็กโทรเคมิคอลสเปคโตรสโกปี ตามลำดับ

สาขาวิชา   วิศวกรรมเคมี   ลายมือชื่อนิสิต ....

ปีการศึกษา   2562   ลายมือชื่อ อ.ที่ปรึกษาหลัก ....

                              ลายมือชื่อ อ.ที่ปรึกษาร่วม ....

6170298021 : MAJOR CHEMICAL ENGINEERING

KEYWORD: CO2 electrochemical reduction; Copper; Electrolyte; Cations; Anions

        Siraphat Somchit : Influences of Cations and Anions in Aqueous Electrolyte on the Electrochemical Reduction of CO_2 over Cu-based Electrode. Advisor: Prof. JOONGJAI PANPRANOT, Ph.D. Co-advisor: Duangamol Tungasmita, Ph.D.

In present work, various aqueous electrolyte solution including Na_2SO_4, NaCl, $NaHCO_3$, K_2SO_4, KCl, $KHCO_3$, Cs_2SO_4, CsCl, and $CsHCO_3$ were employed in the CO_2-ER using Cu-based electrode in an H-cell type reactor. The effects of cations and anions on the production rate were analyzed by GC and NMR. The results showed that electrolyte containing Cl^- as anion not only facilitated CO_2-ER but also suppressed H_2 evolution, the competitive reaction. For the cations effect, rate of CO/H_2 production increased with increasing cation size ($Na^+ < K^+ < Cs^+$). The mixture of HCO_3^- and Cl^- with various ratios (1:1, 1:2, 1:3, and 1:4) were also investigated. It was found that mixed electrolytes can improve the performance of electrolyte. The more Cl^- concentration (0.4M) in mixed electrolyte, the Cu-Cl catalytic film can be presented, which electron transfer is promoted and intermediates can diffuse easier, resulting in the formation of C_2 products. Furthermore, the applied potential in the range of -1.2V to -2.0V vs. Ag/AgCl on CO_2-ER were studied. At higher applied potential, CO intermediates can be further reduced to C_2 products. The electrolyte performances were correlated to the reduction current and resistance of charge transfer (R_{ct}) as revealed by linear sweep voltammetry and electrochemical impedance spectroscopy results, respectively.

Field of Study:	Chemical Engineering	Student's Signature ....
Academic Year:	2019	Advisor's Signature ....
		Co-advisor's Signature ....

ACKNOWLEDGEMENTS

TABLE OF CONTENTS

LIST OF TABLES

จุฬาลงกรณ์มหาวิทยาลัย
CHULALONGKORN UNIVERSITY

LIST OF FIGURES

Chapter I

Introduction

1.1 Introduction

Due to the increase of world energy consumption from a steady growth of industrial sector, the amount of carbon dioxide generated from fossil fuel combustion such as petroleum, natural gas, and coal emitted from industrial and transportation systems also increased. Carbon dioxide is classified as a greenhouse gas, majorly causing global warming. Carbon dioxide can be reduced in many ways including thermochemical, photochemical, biochemical, and electrochemical processes. Electrochemical reduction of CO_2 (ERC) is quite interesting because this reaction can occur at room temperature and atmospheric pressure. Moreover, it can also convert carbon dioxide into value-added products [1].

The main factor that affects ERC is the metal electrodes, which can be divided into 4 groups according to the product selectivity. The 1st group metals are Pb, Hg, In, Sn, Cd, Tl, and Bi, which convert CO_2 to formate as the major product. Au, Ag, Zn, Pd, and Ga, the 2nd group metals, form carbon monoxide as the major product. The 3rd group metal is Cu, it can produce hydrocarbons, alcohols, and aldehydes. The 4th group metals are Ni, Fe, Pt, and Ti, which facilitated hydrogen evolution [2].

Since electrolyte act as an ionic conductor, therefore it also plays an important role in the reaction rate and faradaic efficiency of the ERC. Electrolyte can be classified into 2 types which are aqueous electrolyte and non-aqueous electrolyte. Because of high cost, toxicity and lacking proton donor of non-aqueous electrolyte, therefore performing ERC in the aqueous electrolyte is attractive due to its nontoxicity, wide availability, low price, high sustainability, and availability of proton donors [3].

Because Cu electrode has a moderate binding energy of *CO intermediate, it is the only metal that can provide a wide range of products such as hydrocarbons,

alcohol, and aldehydes [4]. Consequently, this research aims to investigate the effect of cations (Na^+, K^+, Cs^+) and anions (SO_4^{2-}, HCO_3^-, Cl^-) in aqueous electrolyte on ERC process by using Cu as electrode.

1.2 Objective

To study the effect of cations and anions in aqueous electrolyte on the electrochemical reduction of CO_2 over Cu electrode.

1.3 Scope of the research

1.3.1   ERC was performed in an H-cell type reactor. Platinum foil was used as the counter electrode. Ag/AgCl was used as the reference electrode. The working electrode was Cu foil. ERC was performed under room temperature and atmospheric pressure by using various electrolyte including 0.1M Na_2SO_4, 0.1M $NaHCO_3$, 0.1M NaCl, 0.1M K_2SO_4, 0.1M $KHCO_3$, 0.1M KCl, 0.1M Cs_2SO_4, 0.1M $CsHCO_3$, 0.1M CsCl.

1.3.2   The mixture of electrolyte ($KHCO_3$+KCl and $CsHCO_3$+CsCl) with several ratio (1:1, 1:2, 1:3, and 1:4) was also studied in the ERC.

1.3.3   ERC was proceeded under various applied potential (-1.2V vs. Ag/AgCl, -1.4V vs. Ag/AgCl, -1.6V. vs. Ag/AgCl, -1.8V vs. Ag/AgCl, and -2.0V vs. Ag/AgCl) for 70 mins by using the best electrolyte.

1.3.4 CO_2 flow rate before electrolysis was 100 mL/min to achieve the saturated conditions and CO_2 flow rate during electrolysis was 20 mL/min.

1.3.5   Gas products were analyzed by a gas chromatograph equipped with a Shincarbon column and a TCD detector (GC-2014, Shimadzu).

1.3.6   Liquid products were analyzed by a nuclear magnetic resonance (NMR) using phenol and dimethyl sulfoxide (DMSO) as an internal standard.

1.3.7   Characterization of the electrode and electrolyte by various method consists of Physical and Electrochemical techniques including

- Scanning electron microscopy (SEM)
- Linear sweep voltammetry (LSV)
- Electrochemical impedance spectroscopy (EIS)

Chapter II

Literature reviews

2.1 Electrochemical reduction of CO_2 (ERC)

Electrochemical systems focus on the transportation of charge across the interface between chemical phases. Charge is transported through the electrode by the movement of electrons, but it is carried by the movement of ions in the electrolyte phase [5]. There are several ways to reduce CO_2 into valuable products, such as thermochemical reduction, photochemical reduction, biochemical reduction, and electrochemical reduction as shown in Figure 1. The reduction of CO_2 by chemical process requires high temperature and high pressure conditions, thus this method is extremely energy demanding. Biochemical reduction of CO_2 requires bacteria, algae or yeast to produce a specific enzyme, which is used to capture CO_2 and catalyze its reduction to complex molecules. This process is environmentally friendly; nevertheless, it takes a long time to culture bacteria, algae or yeast and it is not stable at extreme temperature and pH value [6]. Photochemical process can convert CO_2 into many valuable products by using solar energy, which is abundant, cheap, and ecologically. However, this method still has some limiting factors, such as narrow light absorption wavelength range, high cost, low activity, and low CO_2 affinity of the photo-catalyst [7].

Electrochemical reduction of CO_2 (ERC) offers an economical and environmentally friendly route for conversion of CO_2 into many valuable products such as hydrocarbon, alcohol or aldehyde. ERC is operated by using electricity as the main source of energy. ERC is an attractive method because this method provides many advantages including [8]:

1. ERC can take place under room temperature and ambient pressure.
2. Wind, solar, hydroelectric, geothermal, or tidal, which is a renewable source of electricity can be used to driven ERC.
3. Easy for scale-up application.

4. High selectivity, low cost of electro-catalyst for conversion of CO_2 into various useful products in aqueous reaction systems.

5. Electrochemical system can be easily decentralized.

6. ERC can be efficiently integrated with photo-reduction to enhance products selectivity.
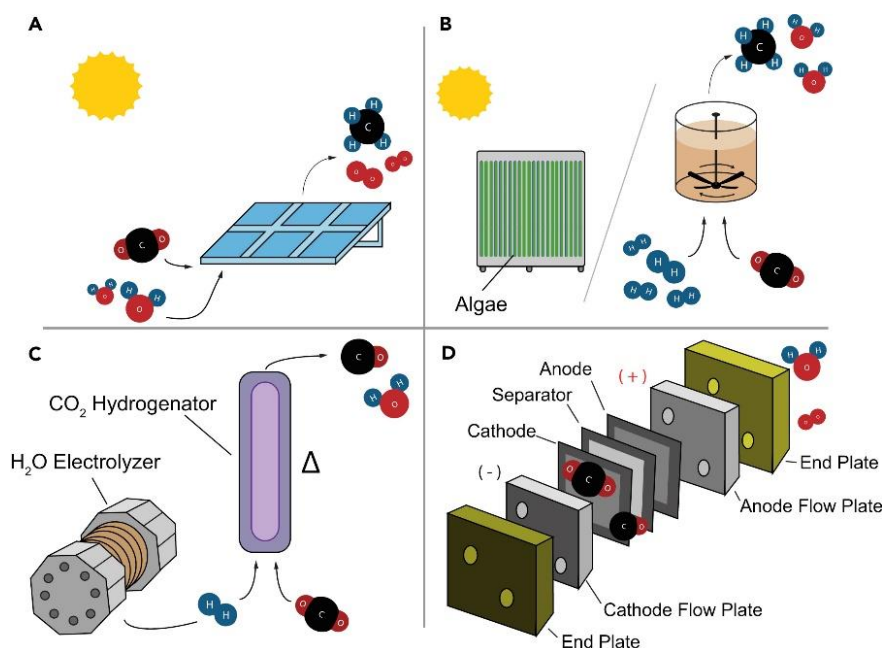
Figure 1 CO_2 conversion processes (A) Photochemical reduction (B) Biochemical reduction (C) Thermochemical reduction (D) Electrochemical reduction [9]

2.2 Fundamental for ERC

Carbon dioxide (CO_2) consists of a carbon atom, which is electrophilic covalently double bonded to two oxygen atoms, which are weak Lewis bases. Reactions of CO_2 are dominated by nucleophilic attacks at the carbon atom, as a result, the O-C-O bond is bent [8]. ERC process requires a voltage source to offer potential (E) to transfer electrons from anode to cathode. The CO_2 electrochemical reduction reaction on a catalyst surface comprises several steps. First, CO_2 transfers from gas phase to the bulk electrolyte. Then, the dissolved CO_2 transport from a bulk electrolyte to the interface between cathode and electrolyte and adsorb at the

cathode surface. After that, the adsorbed CO_2 species dissociate into adsorbed intermediates such as *COOH, *CO, *CHO, and *COH. Then, electron transfer from the working electrode to intermediates. Eventually, products desorb from the electrode and migrate away from the cathode/electrolyte interface to the bulk gas or liquid phase [10].

ERC system consists of three electrodes including (1) working electrode, which CO_2 reduction (Eq.1) occurs. Additionally, hydrogen evolution reaction (HER) (Eq.2) can occur as the competing reaction because ERC and HER take place at the same potential window. (2) Counter electrode, which oxidation of water or normally called oxygen evolution (OER) takes place (Eq.3) [11]. (3) The reference electrode, which is used to standardize the cell [12].

Cathodic reaction:

$$x\text{CO}_2 + n\text{H}^+ + ne^- \rightarrow \text{product} + y\,\text{H}_2\text{O} \qquad \text{CO}_2 \text{ reduction} \quad (1)$$

$$2\text{H}^+ + 2e^- \rightarrow \text{H}_2 \qquad\qquad\qquad \text{H}_2 \text{ evolution} \quad (2)$$

Anodic reaction:

$$2\text{H}_2\text{O} \rightarrow \text{O}_2 + 4\text{H}^+ + 4e^- \qquad\qquad \text{O}_2 \text{ evolution} \quad (3)$$

An excess voltage or overpotential to equilibrium potential (E^0) has to be applied to overcome the energy barrier (resistance) such as ohmic loss from conduction of ions in the bulk electrolytes, ohmic loss from ions transport through membrane or electrical resistance in cell component for driving the ERC reaction [10]. Equilibrium potential E^0 are showed in Table 1.

Table 1 Electrochemical Reaction with Equilibrium Potentials [11]

Reaction	E^0/ [V vs. RHE]	(Product) Name, abbreviation
$2H_2O \rightarrow O_2 + 4H^+ + 4e^-$	1.23	Oxygen Evolution Reaction ,OER
$2H^+ + 2e^- \rightarrow H_2$	0	Hydrogen Evolution Reaction, HER
$xCO_2 + nH^+ + ne^- \rightarrow product + y\,H_2O$	-	CO_2 reduction, CO_2RR
$CO_2 + 2H^+ + 2e^- \rightarrow HCOOH\,(aq)$	-0.12	Formic acid
$CO_2 + 2H^+ + 2e^- \rightarrow CO\,(g) + H_2O$	-0.1	Carbon monoxide
$CO_2 + 6H^+ + 6e^- \rightarrow CH_3OH\,(aq) + H_2O$	0.03	Methanol, MeOH
$CO_2 + 8H^+ + 8e^- \rightarrow CH_4\,(g) + 2H_2O$	0.17	Methane
$2CO_2 + 8H^+ + 8e^- \rightarrow CH_3COOH\,(aq) + 2H_2O$	0.11	Acetic acid
$2CO_2 + 10H^+ + 10e^- \rightarrow CH_3CHO\,(aq) + 3H_2O$	0.06	Acetaldehyde
$2CO_2 + 12H^+ + 12e^- \rightarrow C_2H_5OH\,(aq) + 3H_2O$	0.09	Ethanol, EtOH
$2CO_2 + 12H^+ + 12e^- \rightarrow C_2H_4\,(g) + 4H_2O$	0.08	Ethylene
$2CO_2 + 14H^+ + 14e^- \rightarrow C_2H_6\,(g) + 4H_2O$	0.14	Ethane
$3CO_2 + 16H^+ + 16e^- \rightarrow C_2H_5CHO\,(aq) + 5H_2O$	0.09	Propionaldehyde
$3CO_2 + 16H^+ + 16e^- \rightarrow C_3H_7OH\,(aq) + 5H_2O$	0.10	Propanol, PrOH

Parameters used for electro-catalyst performance analysis

- **Current density (j)** is the total current per geometric surface area of the working electrode, which is used to explain the rate of reaction.

- **Faradaic efficiency (FE)** represents the selectivity of the desired products in a reaction and can be calculated by using Eq. (4)

$$\varepsilon_{FE} = \frac{\alpha nF}{Q} \qquad (4)$$

α = the number of transferred electrons

n = the number of mole of a desired product

F = Faraday's constant (96,485 C/mol)

Q = total charge passed during electrolysis

There are many factors that influence the products selectivity of ERC such as type of metal electrode, type of reactor, electrolyte, reaction conditions, and electrode's surface preparation methods. However, ERC is mainly affected by type of metal electrode and electrolyte.

2.2.1 Type of metal electrode

ERC provides various products, which can be divided into gaseous products and liquid products such as carbon monoxide, methane, formate/formic acid, alcohol, and aldehyde. The product distribution mainly depends on the type of metal electrodes because, the electrode offers the site of the reaction. The product selectivity is affected by the adsorbed molecules and the strength of the adsorption [13]. Electro-catalyst's O and H affinities of electrode affect the binding strength of intermediates, therefore metal electrode can be divided into four groups. The first group consists of Au, Ag, and Zn produce carbon monoxide (CO) as the major product. Because of their lower O and H affinities than Cu, therefore these metals can bind *COOH stronger than *CO, resulting in the easy desorption of CO. The second group, which has higher O affinity, but lower H affinity than Cu including Sn, Pb, In, Hg, Cd, Tl, and Bi. After the reaction step, these metals form *COOH intermediate weakly bound, thus the primary product on these metal surface is $HCOO^-$. Copper (Cu) is the only metal in the 3rd group that not only binds with the $CO_2^{\bullet-}$ intermediate, but also further reduces CO to provide a variety of products such as hydrocarbon, alcohol, and aldehyde. The 4th group metals consist of Ni, Fe, Pt, Ti mainly produced hydrogen (H_2) because of their low hydrogen evolution overpotentials, strong CO adsorption and higher O affinity, H affinity than Cu [12, 14].
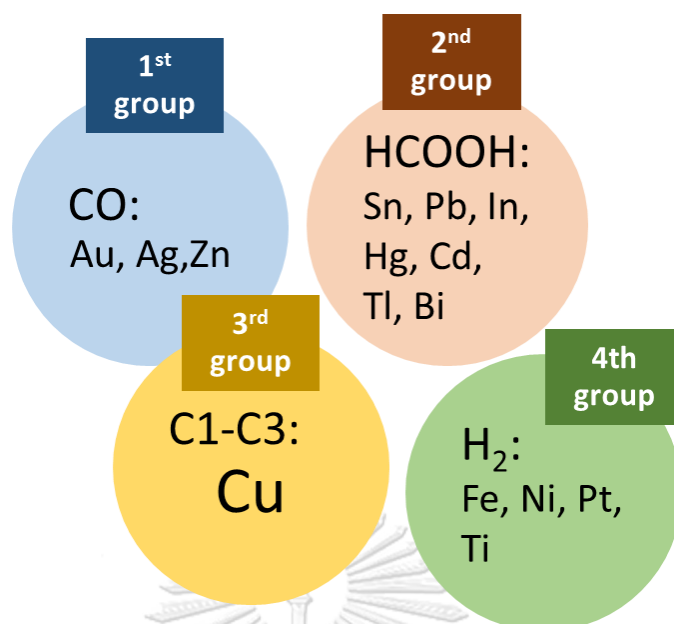
Figure 2 Type of metal electrode

Copper is the only metal that can convert CO_2 into several value-added products such as hydrocarbon, alcohol, and aldehyde. Ren, D. et al. (2018) proposed a mechanism for the formation of products over Cu electrode as shown in Figure 3. The mechanisms can be divided into 2 pathways, including C_1 formation pathway (Fig.3a) and C_2 formation pathway (Fig.3b). For C_1 formation pathway, CO intermediate is reduced to either *OCHO or *COOH via one proton and one electron transfer. After that, *OCHO or *COOH is further reduced to $HCOO^-$ and *CO, respectively. *CO could be additionally reduced to CH_4. For C_2 products pathway, *CO could undergo C-C coupling with another *CO to produce C_2 products, such as ethylene (C_2H_4) and ethanol (C_2H_5OH) [15].
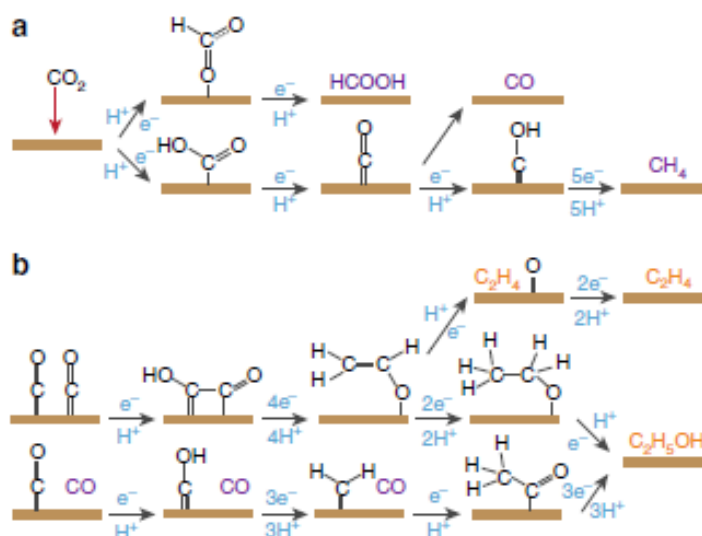
Figure 3 Proposed mechanism for CO_2 electrochemical reduction (a) C_1 formation pathways (b) C_2 formation pathways [15]

2.2.2 Type of electrolyte

Besides type of electrode used, electrolyte also plays an important role in product selectivity and reaction rate. The role of electrolyte in ERC is to conduct ionic charge between electrodes and to transport CO_2 to the cathode active sites. An electrolyte that used in ERC can be divided into aqueous electrolyte and non-aqueous electrolyte. Although aqueous electrolyte has a low solubility of CO_2, performing ERC in aqueous electrolyte provides several benefits; (1) easy to handle and storage (2) low viscosity (3) low price (4) wide availability (5) high sustainability (6) non-toxicity (7) availability of proton donors [3]. An electrolyte used in ERC should be easily dissociated into cations and anions to provide a high ionic conductivity. There have many research focus on the effect of electrolyte on ERC, which can be divided into effect of cations and effect of anions.

Effect of cations

Cations in the electrolyte move towards the negatively charged cathode surface to form an electrical double layer (EDL) as shown in Figure 4. EDL consists of three layers including the outer Helmholtz layer (OHL), inner Helmholtz layer (IHL), and diffuse layer. OHL is the layer that electrostatic adsorption ions are located. IHL is the layer between OHL and electrode surface, which the specifically adsorbed ions, such as halide ions are located. The diffuse layer or bulk region caused by

random motions of ions. The presence of EDL can effect ERC through many mechanisms. For example, the local electrical field between the negatively charged cathode and the positively-charged adsorbed cations has been reported to stabilize CO_2 reduction intermediates such as $*CO_2$ and $*COOH$ [10].
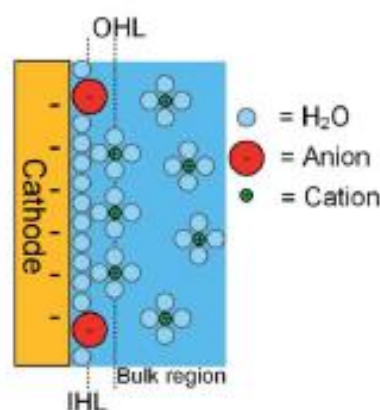
Figure 4 Schematic illustrations of the electrochemical double layer (EDL) [10].

Furthermore, cations size influences the selectivity of products because of its adsorption on the electro-catalyst surface, which alters kinetics and the energy required in the electrochemical reaction [16]. In 1991, Murata, A. and Hori, Y. studied the effect of cation in an aqueous electrolyte by using HCO_3^- as anion on product selectivity of electrochemical reduction of CO_2 over Cu electrode. The results showed that electrolyte containing Li^+ facilitated H_2 evolution, the side reaction, whereas CO_2 reduction was favorable in Na^+, K^+, and Cs^+ solutions. Ethylene (C_2H_4) production became more than CH_4 with increasing cation size. It was found that cationic species influenced the product selectivity due to the varying of the outer Helmholtz plane (OHP) potential. Consequently, the concentration of H^+ at the electrode changed because of the changing in OHP potential, resulting in the difference of pH at the electrode, which can alter products selectivity [17]. In 2012, the effect of electrolyte including $KHCO_3$, K_2SO_4, KCl, Na_2SO_4, Cs_2SO_4, $NaHCO_3$, and $CsHCO_3$ on ERC were investigated by Wu, J. et al. over Sn electrode. Na_2SO_4 exhibited the highest faradaic efficiency of formate and the highest energy efficiency, while $KHCO_3$ exhibited the highest rate of formate production. Furthermore, concentration of electrolyte also affected formate selectivity. The formate selectivity increased with decreasing electrolyte concentration. They found that the Sn electrode was

degraded after 10 hour electrolysis due to the electrodeposition of the trace amounts of Zn in electrolyte, which was confirmed by SEM-EDX and XPS. [18]. In 2016, Singh, M. et al. reported that the pK_a for cation hydrolysis decreased with increase alkaline cation size, resulting in K^+, Rb^+, Cs^+ serve as buffering agents. Buffering caused the pH near cathode lower, led to an increasing in the local concentration of dissolved CO_2. Due to an increasing of the local concentration of dissolved CO_2, the faradaic efficiency for CO, C_2H_4, and C_2H_5OH increased with increasing alkaline cation size [19]. Lum, Y. et al. (2017) prepared four different oxide-derived copper for electrochemical reduction of CO_2 including oxide-derived nanocrystalline copper, copper nanowire arrays, electrochemically cycled copper, and reduced electrodeposited Cu(I) oxide film and varying electrolyte used in reaction consists of $KHCO_3$ and $CsHCO_3$. $CsHCO_3$ showed a higher selectivity of C_{2+} products than $KHCO_3$. They demonstrated that high selectivity of C_{2+} products can be achieved by a high local CO_2 concentration, which can be done by operating at a current density sufficiently high to achieve a moderately high pH near the catalyst surface but not too high to cause a significant decreasing in the local concentration of CO_2 [20].

Effect of anions

Anions present different buffer capacities, which led to different local pH. The difference in local pH influences the availability of proton, therefore, affects the reaction kinetics such as the binding strength or adsorption geometry of CO_2 electrochemical reduction intermediates. In 2010, Ogura, K. et al. demonstrated that halide ions (Cl^-, Br^-, I^-) enhanced the rate of electrochemical CO_2 reduction and suppressed the hydrogen evolution, the competing reaction over Cu mesh electrode because of the presence of Cu-X (X= Cl^-, Br^-, I^-) catalytic layer, which facilitated the electron transfer from the electrode to CO_2 [21]. In 2018, Huang, Y. et al. investigated the effect of anions ($KClO_4$, KCl, KBr, KI) on ERC using Cu as the working electrode. KI achieved 50% selectivity of ethylene and 16% selectivity of ethanol. The favorable CO_2 reduction to C_{2+} products corresponded to a higher *CO population on the surface, which was confirmed by linear sweep voltammetry (LSV) technique. Moreover, Raman spectroscopy evidenced that the coordination environment of *CO

was changed by anions. They concluded that anions play an important role in enhancing the formation of C_{2+} products by tuning the coordination environment of adsorbed *CO, which can improve C-C coupling [22]. In the same year, Nguyen, D.L.T. et al. studied the electrochemical reduction of CO_2 over Zn-based electrode by using an electrolyte containing different halide ions (F^-, Cl^-, Br^-, I^-) and using K^+ as cation. The result showed that the presence of halides ion presented the high electro-catalytic performance of CO_2 reduction and suppression of hydrogen evolution, the competing reaction with a maximum CO faradaic efficiency 97%. They discovered that the increasing of adsorption strength from F^- to I^- was proposed to form more porous structures and higher oxidized Zn species, therefore facilitating the protonation of CO_2 and stabilizing the adsorbed intermediates induced by charge donation from the adsorbed halides on Zn surface to CO_2, enhance CO_2 electrochemical reduction and suppress HER at the same time [23].

Because HCO_3^- can act as a buffering agent and can be a CO_2 reservoir [3]. Halide ions increased CO_{ads} coverage on the electro-catalyst surface and stabilizing intermediates, therefore they facilitated CO_2 reduction and simultaneously suppressed hydrogen evolution, the competing reaction. Consequently, there has research about mixture electrolytes to improve electro-catalytic performance. In 2016, Varela, A. et al reported that the activity and selectivity of copper during CO_2 electrochemical reduction can be adjusted by adding halides ion to an electrolyte containing HCO_3^-, thus they studied the effect of mixing electrolyte by adding several halide ions including Cl^-, Br^-, and I^-. Addition Cl^- and Br^- enhanced CO selectivity, whereas I^- decreased CO selectivity, but increased CH_4 selectivity. These results were mainly correlated to halides adsorption on Cu electrode surface. Moreover, they hypothesized that the increasing of negative charge by adding halides adjusted the electro-catalytic performance of Cu [24]. In 2017, Hong, S. et al. studied the effect of anions (Cl^-, SO_4^{2-}, HPO_4^{2-}, HCO_3^-) on the CO/H_2 production over Au sputtered on a gas diffusion layer (GDL) electrode. HCO_3^- was mixed with each electrolyte to keep the bulk pH constant during electrolysis. It was found that CO/H_2 ratio increased by using Cl^- as anion because of the strongly adsorbed. HPO_4^{2-} exhibited the minimum CO faradaic efficiency (11%), but the maximum H_2 faradaic efficiency (70%). They

concluded that the product distribution was depended on the specific adsorption strength and intrinsic characteristic of anions, which was confirmed by many analytical tools including LSV, EIS, SEM, XPS, and XRD [25].

2.3 Electrochemical techniques

2.3.1 Linear sweep voltammetry (LSV)

Linear sweep voltammetry (LSV) is widely used because it requires simple and inexpensive instrumentation. In an LSV technique, the potential is swept linearly from an initial (V_1) to final values (V_2) with a constant scan rate as shown in Figure 5 and the current is measured as a function of time. The result from LSV is the plot between current and potential (I-V curve). [26]
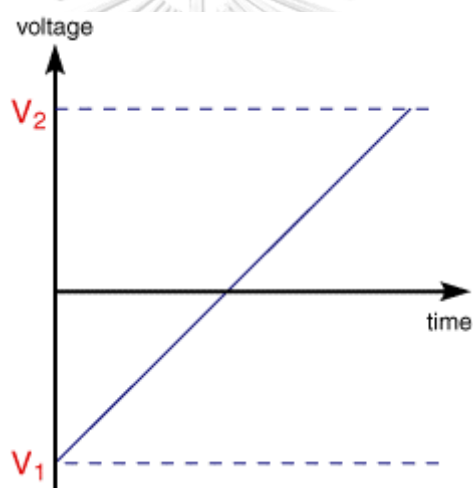
Figure 5 Linear sweep voltammetry [27]

LSV technique provides information not only on the electrochemical of redox reactions but also chemical reactions integrated with charge transfer steps. This electroanalytical technique is usually used to examine the kinetics of electron transfer reactions including catalysis and has been expanded for use in organic and inorganic synthesis, sensor, and physical mechanics of electron transfer reaction. Moreover, it can provide the onset potential, which is the potential that the electrochemical reaction occurs. [28]

2.3.2 Electrochemical impedance spectroscopy (EIS)

Electrochemical impedance spectroscopy (EIS) is an electroanalytical method that widely used as a standard characterization technique for many material

systems and applications such as batteries, plating, and corrosion. It is a very useful technique for analyzing the characteristics of an electrochemical system because it can separate the influence of physical characteristics and electrochemical phenomena at a constant potential. [29]

In EIS technique, an alternating current or potential perturbation signal in a sinusoidal waveform was applied to the cell and the current or potential response over the high frequencies to the low frequencies was measured. EIS can provide many information about electrochemical system such as the solution resistance (R_s), charge transfer resistance (R_{ct}) and the diffusion phenomena. [30]

The plot of the relation between the real part and the imaginary part of the impedance is called the Nyquist plot as shown in Figure 6. The advantage of the Nyquist plot is that it can provide a quick overview of the data and can also be explained qualitatively. The shape of the graph is important in the qualitative interpretation of the data.

Normally, the experimental impedance of an electrochemical system consists of electrolysis cells, potentiostat, and frequency response analyzer (FRA). The most widely used electrolysis cell is a three electrode system cell that including the working electrode (WE), which is the electrode under analysis, the electrode that makes the complete electrical circuit is called the counter electrode (CE), and the reference electrode (RE) that is used to determine the electric potential of the working electrode to be certain. [31]
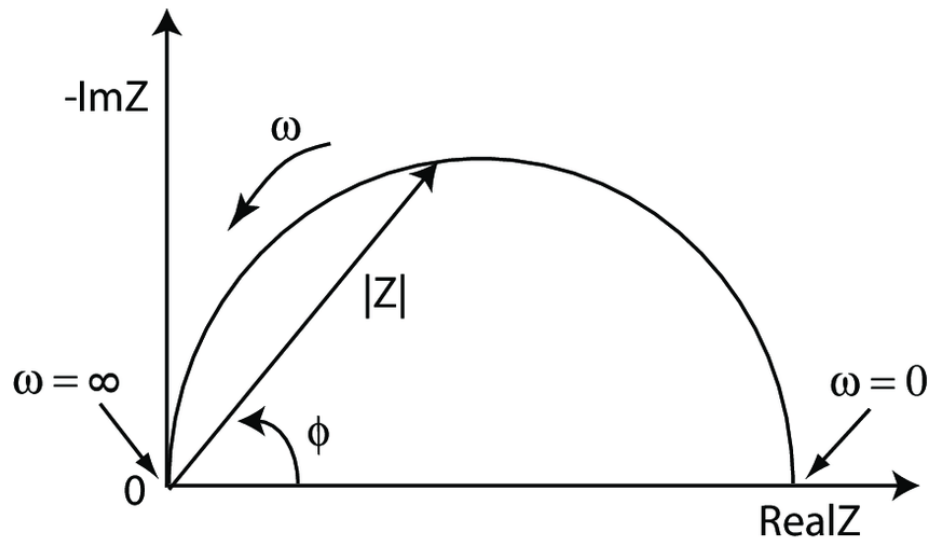
Figure 6 Generally Nyquist plot [32]

Chapter III

Experimental

3.1 Materials

Working electrode and counter electrode including copper foil (thickness 0.1mm, 99.9999%) and platinum foil (thickness 0.1mm, 99.997%) were obtained from Alfa Aesar. Ag/AgCl, which was used as the reference electrode was acquired from Metrohm. All electrolyte used in the experiment consisting of Na_2SO_4, $NaHCO_3$, NaCl, K_2SO_4, $KHCO_3$, KCl, Cs_2SO_4, $CsHCO_3$, CsCl were purchased from Sigma-Aldrich. Nafion117 membrane, which was used to separate cathode and anode compartments was procured from Aldrich. CO_2 (99.8% purity) was purchased from Linde.

3.2 Electrode surface preparation

Before electrolysis, Cu foil was mechanically polished with sandpaper 2500G until no discoloration was visible and then rinsed with DI water. Finally, the Cu foil was dried under N_2.

3.3 Electrochemical test

ERC was performed in an H-cell type reactor as shown in Figure 7. The working electrode was Cu foil which had a surface area 1x1 cm^2. Pt foil was used as the counter electrode. Ag/AgCl was used as the reference electrode. A Nafion 117, proton exchange membrane was used to separate anode and cathode compartments and to prevent the anion liquid products such as acetate and formate crossover to the anode compartment [33]. Nafion membrane has to be pretreated prior used in the reaction to remove the impurities. First, it was treated with 1M H_2SO_4 at 80^oC for 1h. Then, it was boiled in DI water for 1h. After that, it was treated with 3% H_2O_2 at 80^oC for 1h. Finally, it was boiled in DI water for 1h and stored in the electrolyte or DI water at least 12h before the experiment takes place [34]. Before electrolysis, CO_2 gas was bubbled through the electrolyte with flowrate 100 mL/min until saturated conditions. After saturated, CO_2 gas was continuously bubbled with flowrate 20 mL/min during electrolysis. Then, the electrolysis was proceeded under a constant potential (-1.2V vs. Ag/AgCl, -1.4V vs. Ag/AgCl, -1.6V vs. Ag/AgCl, -1.8V vs.

Ag/AgCl, -2.0V vs. Ag/AgCl) for 70 minutes by employing a potentiostat. The electrolyte investigated in this work including Na_2SO_4, NaCl, $NaHCO_3$, K_2SO_4, KCl, $KHCO_3$, Cs_2SO_4, CsCl, $CsHCO_3$, and the mixed electrolyte with several ratios (1:1, 1:2, 1:3, and 1:4).
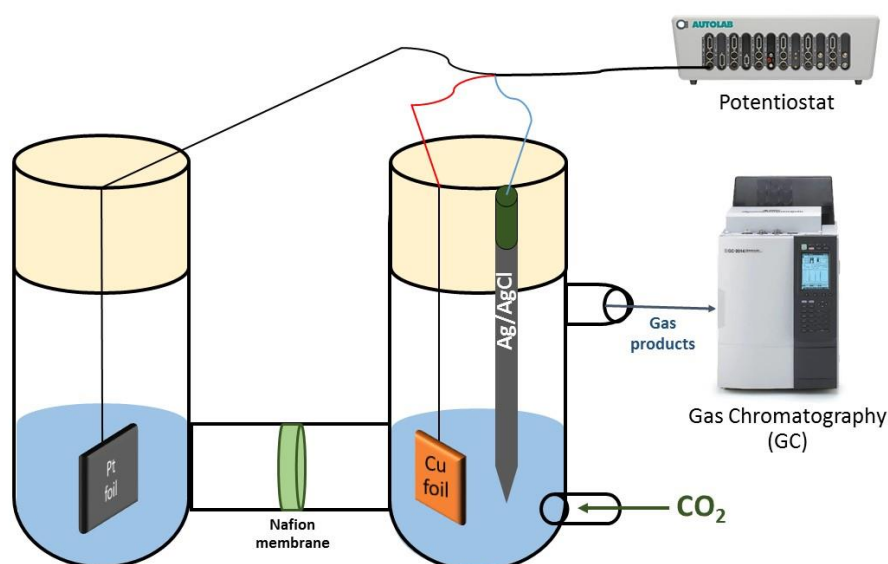
Figure 7 CO$_2$ electrochemical reduction performed in an H-cell reactor

3.3 Products analysis

Gas products were analyzed by a gas chromatograph (GC) equipped with a Shincarbon column and a TCD detector (GC-2014, Shimadzu). Liquid products were quantified by Nuclear Magnetic Resonance (NMR). To determine liquid products, sampling liquid containing CO_2 reduction products 400 microliters and then mixed with dimethyl sulfoxide (DMSO) and phenol, which was used as an internal standard. After that, deuterium oxide (D_2O) was added as a solvent for NMR analysis.

3.4 Characterization

3.4.1 Physical characterization

Scanning Electron Microscope (SEM)

The morphology of the working electrode's surface before and after mechanically polishing was investigated by scanning electron microscope (SEM).

3.4.2 Electrochemical measurement

Linear sweep voltammetry (LSV)

Linear sweep voltammetry is a voltammetric method where the current at a working electrode is measured while the potential between the working electrode and the reference electrode is swept linearly in time. This method was used to determine the applied potential that CO_2 electrochemical reduction would occur [35]. In this work, potential sweep linearly from 0V to -2.0V vs. Ag/AgCl with a scan rate of 50 mV/s.

Electrochemical Impedance Spectroscopy (EIS)

The EIS is a widespread experimental technique, which is used to characterize the behavior of an electrochemical system. EIS was carried out with Nova software potentiostatic EIS mode in the frequency range 5,000 – 0.1 Hz at the operating applied potentials. This technique was employed to determine the electrolyte conductivity and electron conductivity of each electrolyte.

จุฬาลงกรณ์มหาวิทยาลัย

CHULALONGKORN UNIVERSITY

Chapter IV

Results and Discussion

In this chapter, the performance of electrolytes over Cu electrode is discussed. The results and discussion are divided into three parts. Firstly, the investigation of single electrolytes including the effect of cations (Na^+, K^+, Cs^+) and effect of anions (SO_4^{2-}, HCO_3^-, Cl^-) for CO_2 electrochemical reduction are reported. Secondly, the study of mixing ratio (1:1, 1:2, 1:3, and 1:4) of mixed electrolytes ($KHCO_3$+KCl and $CsHCO_3$+CsCl) are demonstrated. Finally, the effects of the applied potentials (-1.2V vs. Ag/AgCl, -1.4V vs. Ag/AgCl, -1.6V vs. Ag/AgCl, -1.8V vs. Ag/AgCl, and -2.0V vs. Ag/AgCl) on the electrochemical reduction of CO_2 are discussed.

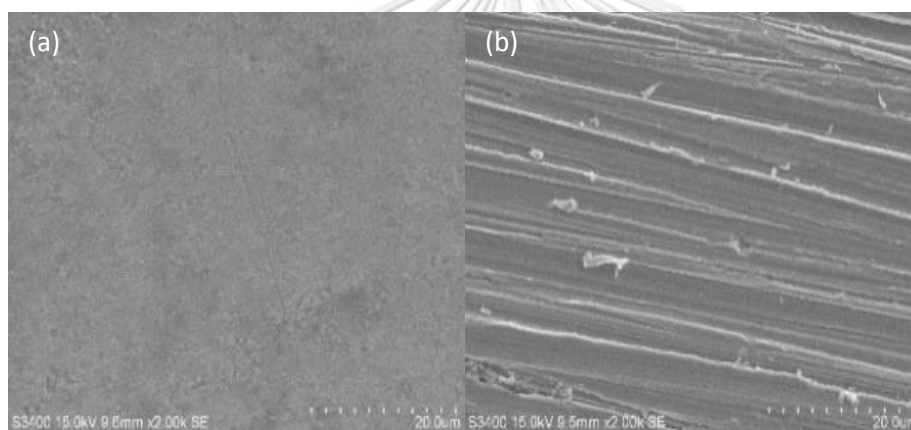## 4.1 Electrode surface characterization

Figure 8 SEM image of copper foil (a) before; (b) after mechanically polishing

SEM images of the copper electrode are shown before mechanically polishing (Figure 8a) and after mechanically polishing (Figure 8b). As can be seen from these figures, the surface of copper electrode became more rough after mechanical polishing.

4.2 Electrochemical reduction of CO_2

4.2.1 Part I Effect of cations and anions in aqueous electrolyte

Table 2 pH of each electrolyte before and after saturation with CO_2

Electrolyte	pH without CO2	pH with CO2 sat.	ΔpH
Na_2SO_4	7.45	4.65	2.80
$NaHCO_3$	8.97	6.94	2.03
NaCl	7.58	4.34	3.24
K_2SO_4	6.80	4.68	2.12
$KHCO_3$	9.16	7.04	2.12
KCl	7.68	4.19	3.49
Cs_2SO_4	7.42	4.84	2.58
$CsHCO_3$	9.43	7.18	2.25
CsCl	7.74	4.33	3.41

From Table 2, pH of all electrolytes decreased when CO_2 was purged into the electrolyte because of the acidity of the gaseous CO_2. The difference of pH between without CO_2 and CO_2 saturated shows the solubility of CO_2 in electrolyte. For all cations, electrolyte that containing Cl^- as anion shows the highest CO_2 solubility compared to other anions, which is corresponded to CO_2 reduction products formation as shown in Table 4. Although NaCl exhibited the solubility of CO_2 more than $NaHCO_3$, NaCl produces CO formation less than $NaHCO_3$. This may be caused by the extremely dissolution of NaCl, which can be induced to salting-out effect. The NaCl presented the higher K_{sp} than Na_2SO_4 and $NaHCO_3$, respectively (37.95 > 7.74 > 1.50) [36]. The higher value of K_{sp}, demonstrating the higher salt dissociation, which can hinder the movement of CO_2 to the copper electrode [37].

Before electrolysis, linear sweep voltammetry (LSV) technique was used to determine the onset potential, which is the applied potential that CO_2 electrochemical reduction would occur. The onset potential is the potential that the current density under CO_2 saturated conditions began to increase significantly. The onset potential of each electrolyte can be seen in Table 3.
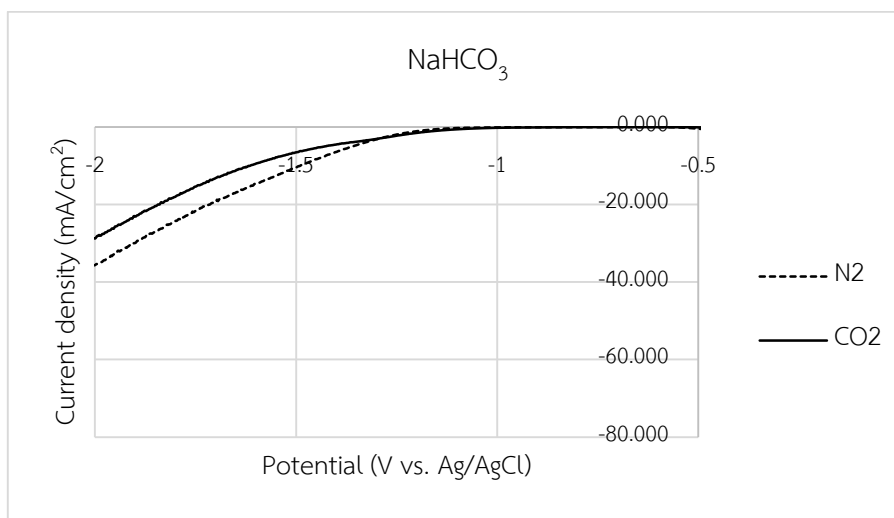
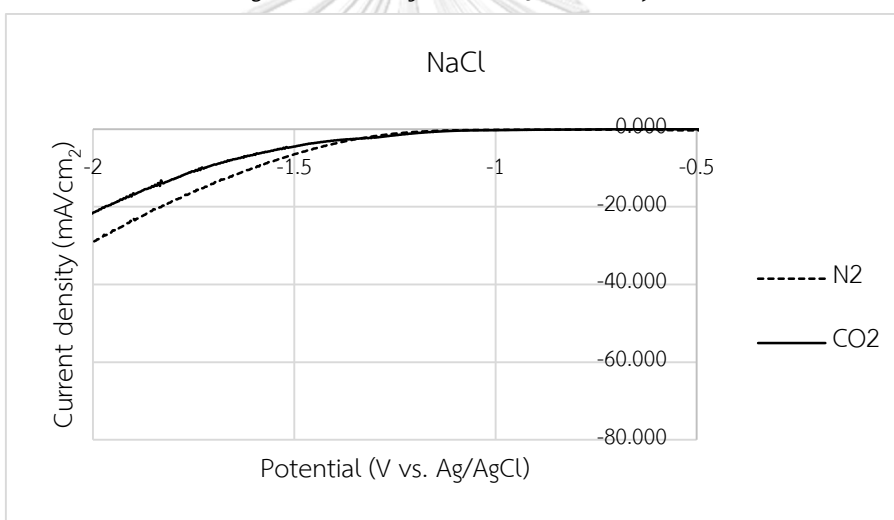*Figure 9 LSV of NaHCO₃ electrolyte*

Figure 10 LSV of NaCl electrolyte
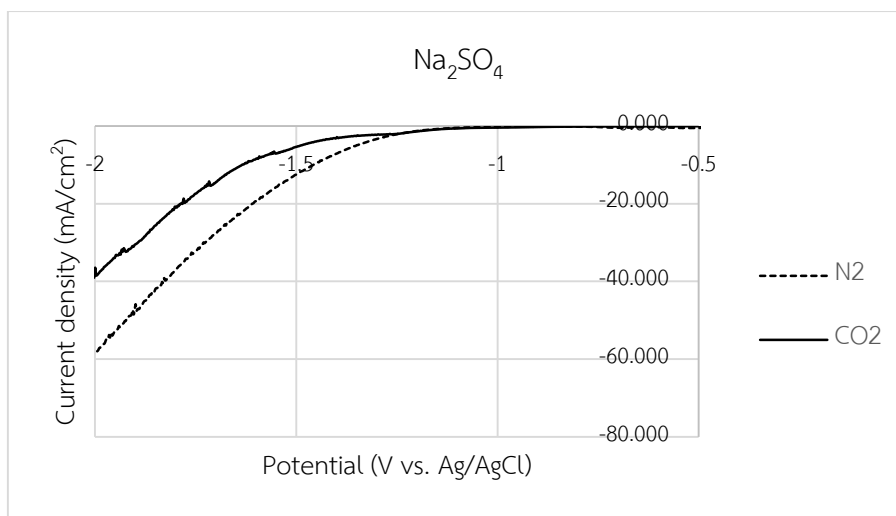
Figure 11 LSV of Na₂SO₄ electrolyte
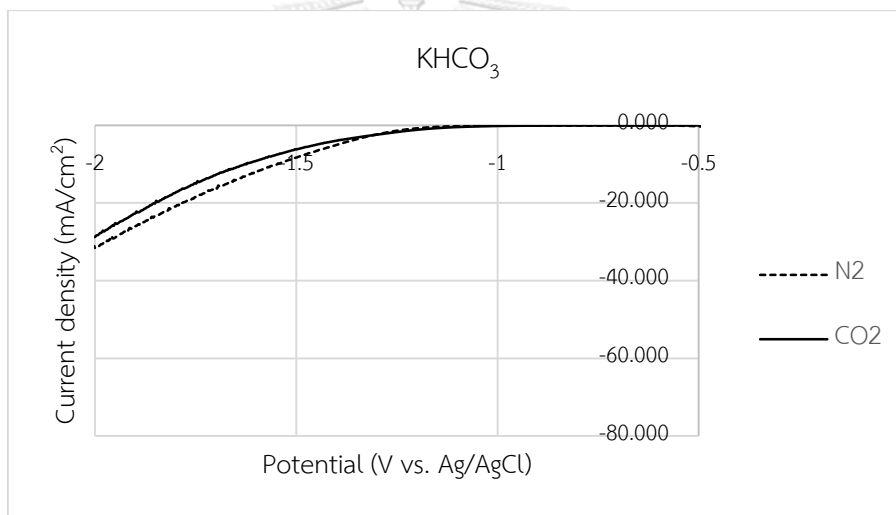
Figure 12 LSV of KHCO₃ electrolyte
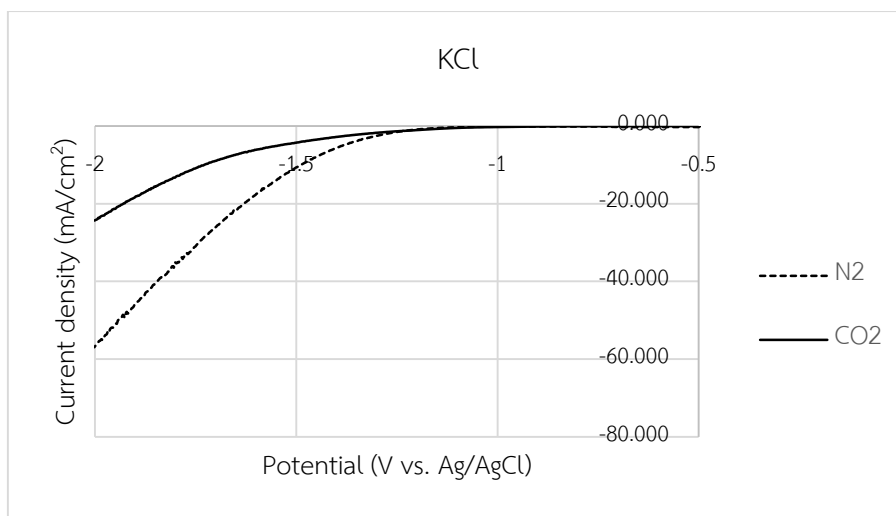
Figure 13 LSV of KCl electrolyte
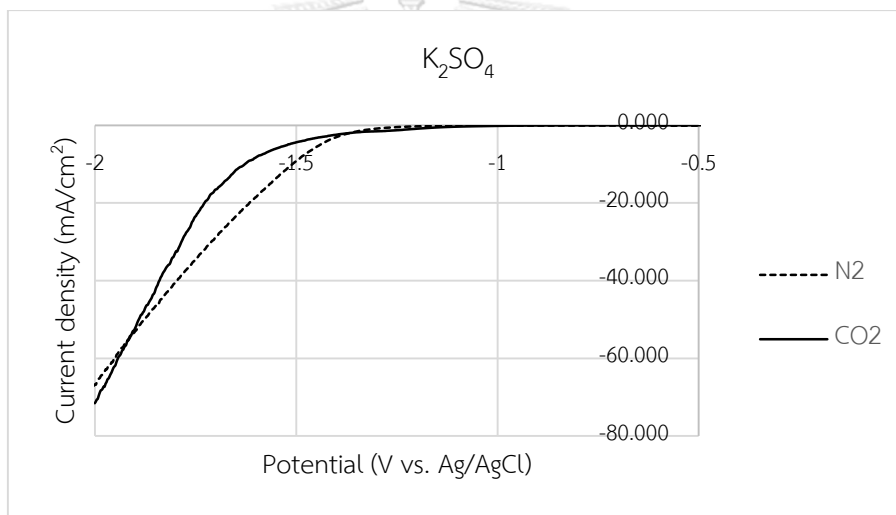
Figure 14 LSV of K_2SO_4 electrolyte
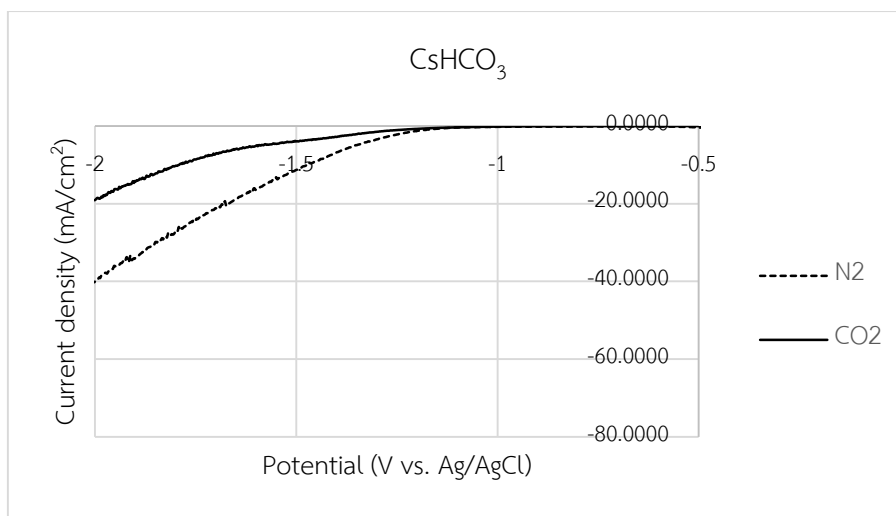
Figure 15 LSV of CsHCO₃ electrolyte
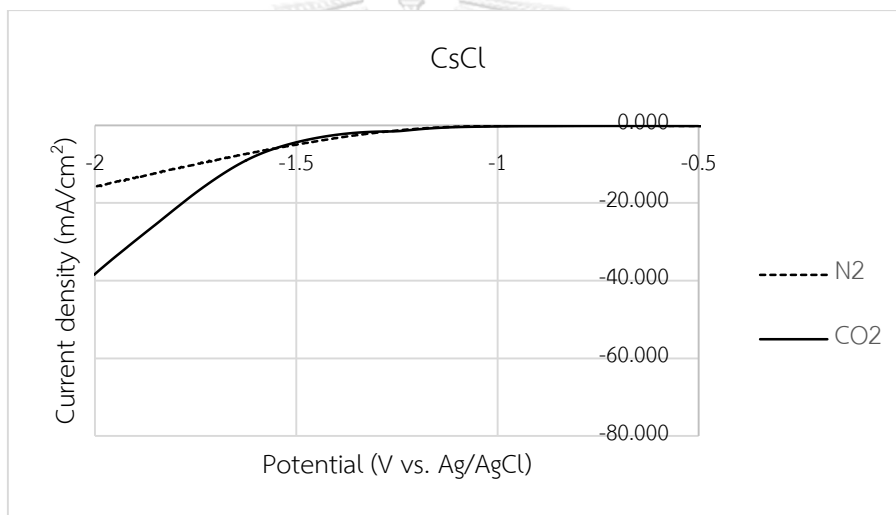
Figure 16 LSV of CsCl electrolyte
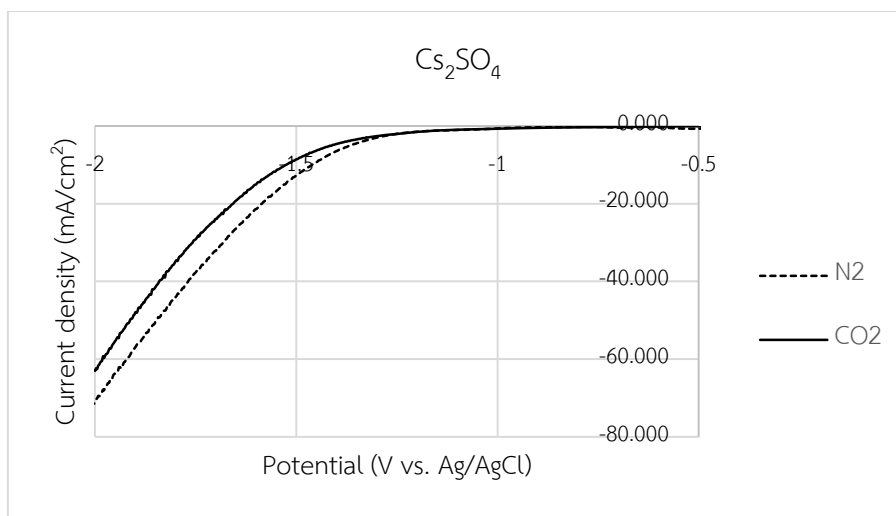
Figure 17 LSV of Cs$_2$SO$_4$ electrolyte

Table 3 The onset potential of each electrolyte

Electrolyte	Onset potential (V vs. Ag/AgCl)
Na$_2$SO$_4$	-1.40
NaHCO$_3$	-1.42
NaCl	-1.43
K$_2$SO$_4$	-1.50
KHCO$_3$	-1.40
KCl	-1.40
Cs$_2$SO$_4$	-1.40
CsHCO$_3$	-1.40
CsCl	-1.60

Since the applied potential at -1.60V vs. Ag/AgCl was the potential that CO$_2$ electrochemical reduction can take place in all electrolytes, the applied potential -1.6V vs. Ag/AgCl was chosen to study the performance of each electrolyte.

Table 4 Rate of CO$_2$ reduction products from ERC of each electrolyte

Electrolyte	Rate of gas products (µmol/min)			Rate of liquid products (µmol/min)	
	CO	H$_2$	CO/H$_2$	Formate	Ethylene glycol
Na$_2$SO$_4$	0.016	7.218	0.002	0.224	0
NaHCO$_3$	0.201	2.670	0.075	0.161	0
NaCl	0.144	2.571	0.056	0.233	0
K$_2$SO$_4$	0.246	3.362	0.073	0.234	0.064
KHCO$_3$	0.274	1.710	0.160	0.167	0
KCl	0.348	2.637	0.132	0.343	0
Cs$_2$SO$_4$	0.288	2.604	0.111	0.069	0.043
CsHCO$_3$	0.294	2.439	0.121	0.360	0
CsCl	0.300	1.417	0.212	0.201	0

From Table 4, carbon monoxide (CO) and formate (HCOO$^-$) were observed as a major CO$_2$ reduction products for all electrolytes because these products can be produced more easily than the other products due to the requirement of only 2 electrons transfer [38]. Electrolyte containing SO$_4^{2-}$ as anion (K$_2$SO$_4$ and Cs$_2$SO$_4$) can reduce CO$_2$ into ethylene glycol as a minor product which may be due to the lower pH of the electrolyte that contains SO$_4^{2-}$, which facilitates the production of glyoxal, the intermediate reagent to ethylene glycol [39]. Meanwhile, Cl$^-$ also exhibited a lower pH value but ethylene glycol cannot be detected. This maybe because of the specific adsorption of Cl$^-$ on Cu electrode during the reaction, which can stabilize intermediate species [40] so that they become more difficult to desorb.

Although some electrolytes produce a high rate of CO production, they also produce a high rate of H$_2$ evolution, the undesired product as well. In order to be able to compare the performance of an electrolyte, the rate of CO/H$_2$ production was calculated.

As can be seen from Table 4, CsCl not only exhibited the highest rate of CO/H_2 production but also exhibited the lowest rate of H_2 production. Comparing the effect of cations (NaCl, KCl, CsCl), the rate of CO/H_2 increased with increasing cation size. For the anions effect (Cs_2SO_4, $CsHCO_3$, CsCl), Cl^- showed the maximum rate of CO/H_2 production as shown in Table 4. SO_4^{2-} and HCO_3^- produced resemble rate of CO/H_2 production.

Because ERC was performed in an aqueous electrolyte, hydrogen evolution reaction (HER) is usually occur as the competitive reaction against ERC. Therefore, controlling activity of HER is one of many procedures to increase the rate of CO/H_2 production. For the cations effect, rate of H_2 production decreased with increasing cation size. For anions effect, electrolyte containing SO_4^{2-} showed the highest rate of H_2 production. Cl^- exhibited the lowest H_2 production rate.

From LSV results (Figure 9-17), the presence of only N_2 saturation represents the hydrogen evolution reaction (HER) because no CO_2 was fed into the system. As can be seen from Figure 11, 14, and 17 the highest value of current density under N_2 saturation was obtained by the electrolyte containing SO_4^{2-} for all cations. The highest value of the current density demonstrates the highest speed of electrons transfer, resulting in the maximum H_2 production. Moreover, the pH value under CO_2 saturated conditions of SO_4^{2-} electrolyte is a quite acidic solution, which promotes the HER [41]. Whereas the pH value of Cl^- containing electrolyte is quite acidic solution as well, however, Cl^- is more strongly adsorbed on the Cu electrode than SO_4^{2-}. Therefore, it can block reactive sites for HER [24]. CO_2 saturated conditions represents the HER and ERC [21]. CsCl shows the higher current density under CO_2 saturated conditions than N_2 saturated conditions, indicating that CsCl favors CO_2 reduction more than H_2 evolution.

Because CsCl exhibited the highest rate of CO/H_2 production, therefore Cs^+ cation is fixed to study the effect of anion including SO_4^{2-}, HCO_3^- and Cl^-. Meanwhile, Cl^- anion is fixed to investigate influence of cation consisting of Na^+, K^+, Cs^+.
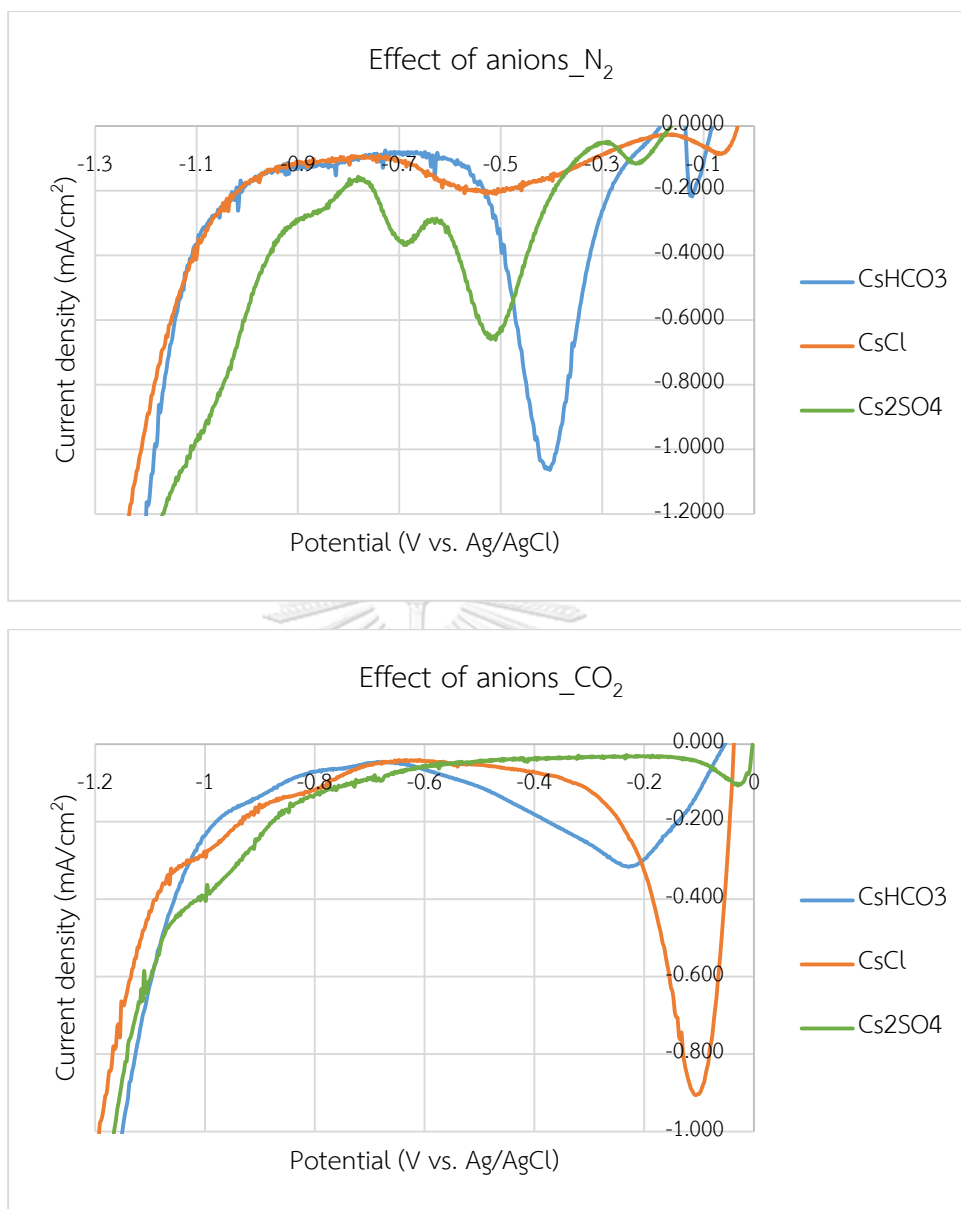
Figure 18 LSV of CsHCO₃, CsCl and Cs₂SO₄ under N₂ saturation (a) CO₂ saturation (b)

Figure 18(a) shows the LSV of $CsHCO_3$, CsCl and Cs_2SO_4 under N_2 saturated conditions. The first reduction peak located at -0.1V vs. Ag/AgCl, suggests that the CuO reduces to Cu [42]. The second peak located at -0.4V vs. Ag/AgCl appears when using $CsHCO_3$ electrolyte, indicating that the HCO_3^- anion from electrolyte is directly reduced to formate [43], resulting in the maximum rate of formate production. CsCl and Cs_2SO_4 have a signal at -0.5V vs. Ag/AgCl, which corresponded to the proton reduction peak [44], and cannot be seen in the presence of CO_2. Since, $CsHCO_3$ shows a broad peak for HCO_3^- reduction, the proton reduction signal can be

overlayed. CsCl shows the lowest proton reduction current, indicating that Cl^- anion can suppress the HER more than other anions. It was found that only when SO_4^{2-} is presented, a reduction peak at -0.7V vs. Ag/AgCl, which could be ascribed to the adsorption of sulfate. Figure 18(b) shows LSV of $CsHCO_3$, CsCl and Cs_2SO_4 under CO_2 saturated conditions. The sharp reduction peak located at -0.1V vs. Ag/AgCl, could be corresponded to CuO to Cu [42] and adsorbed CO formation on electrode surface [45] because of the higher current density. $CsHCO_3$ presents a broader peak due to the combination of CuO reduction, adsorbed CO formation, and HCO_3^- reduction peaks. The current density increased in order: SO_4^{2-} < HCO_3^- < Cl^-, the more current density means that more CO adsorbed on the electrode surface, resulting in the highest CO formation when using Cl^- as anion.
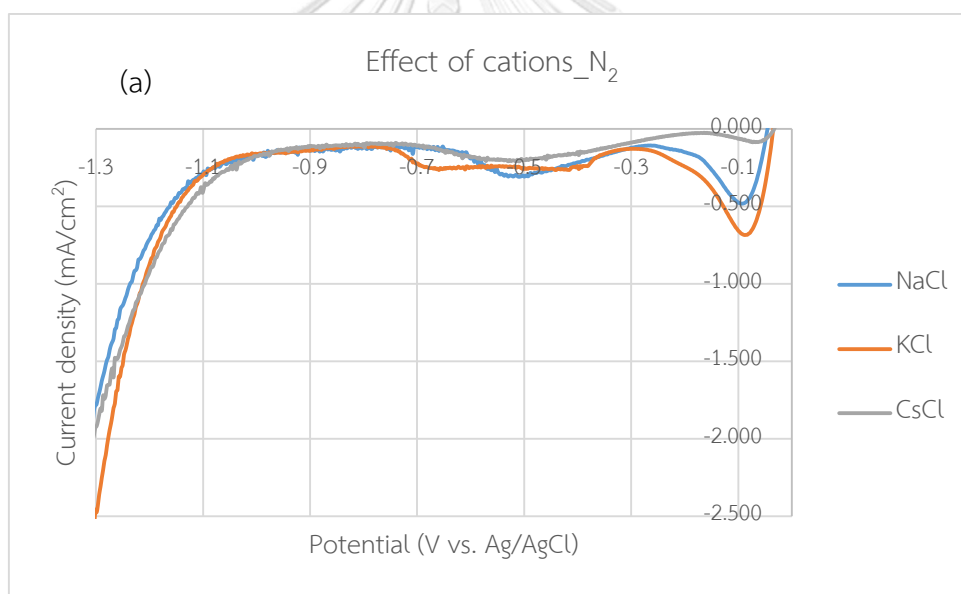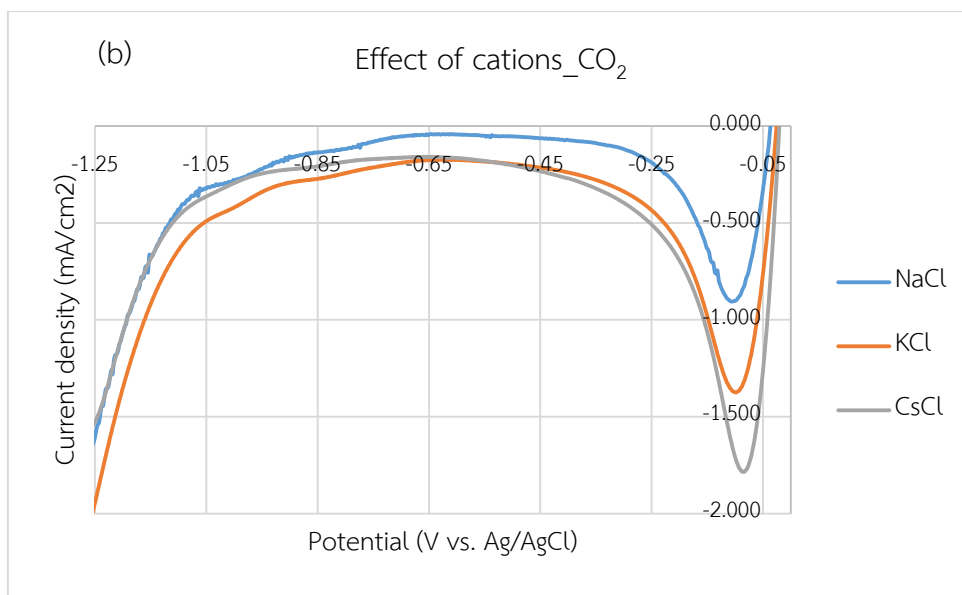
Figure 19 LSV of NaCl, KCl and CsCl under N$_2$ saturation (a) CO$_2$ saturation (b)

From Figure 19(a), the first peak shows the reduction of oxide on the Cu electrode's surface [42]. The second peak locates at -0.5V vs. Ag/AgCl, which is attributed to the proton reduction peak [44]. For K$^+$ cation, the proton reduction peak might be shifted to -0.7V vs. Ag/AgCl. The proton reduction current increases with decreasing cation size in order: Cs$^+$ < K$^+$ < Na$^+$, showing that Na$^+$ cation can reduce proton faster than K$^+$ and Cs$^+$, resulting in the highest H$_2$ evolution. Figure 19(b) shows LSV of NaCl, KCl and CsCl under CO$_2$ saturation, there are only reduction peaks located at -0.1V vs. Ag/AgCl. The signal was attributed to CuO reduction to Cu [42] and the formation of adsorbed CO [45]. The reduction current of Cs$^+$ and K$^+$ are not significantly different in accordance with rate of CO formation. Na$^+$ cation exhibited the lowest current density, indicating that the lowest of adsorbed CO formation on the electrode, resulting in the lowest CO production. Furthermore, Murata, A. and Hori, Y. suggested that that bigger cation size, the less hydration number, resulting in the more amount of cation adsorbed on the electrode. The greater cation specifically adsorb on the electrode can block the sites for HER [17] and lead to a larger interaction between electrode and hydrated cations, which drives the adsorption of CO$_2$ [46]. Although the larger surface charge density of Cs$^+$ can drive the adsorption of CO$_2$, Cs$^+$ exhibited CO and formate formation less than

K^+. This may be caused by the more adsorption propensity of Cs^+ may have reduced available reaction sites for CO_2 reduction intermediates as well [30].

4.2.2 Part II Effect of mixing ratio of mixed electrolytes

Because electrolyte containing Na^+ as cation and SO_4^{2-} as anion abundantly produce H_2, the undesired product. Cl^- was the best anion in part I that produce the highest rate of CO_2 reduction products and the lowest rate of H_2. Furthermore, HCO_3^- can act as a buffering agent and can be CO_2 reservoir [3]. Therefore, in this part $KHCO_3+KCl$ and $CsHCO_3+CsCl$ were chosen to study with several mixing ratio.

Table 5 pH of each electrolyte with several ratios before and after saturation with CO_2

Electrolytes	Ratio	pH without CO_2	pH with CO_2 sat.	ΔpH
$KHCO_3$:KCl	1:1	9.47	7.10	2.37
	1:2	9.06	7.06	2.02
	1:3	9.07	7.01	2.06
	1:4	9.30	6.99	2.31
$CsHCO_3$:CsCl	1:1	9.08	7.08	2.00
	1:2	9.14	7.02	2.12
	1:3	9.12	6.99	2.13
	1:4	9.15	6.97	2.18

Table 5 shows the pH value of mixed electrolyte with various ratio, the pH value with CO_2 saturated conditions is not significantly different due to the buffer ability of HCO_3^- [25]. Moreover, pH of all ratios decreased in the presence of CO_2 because of the acidity of the gaseous CO_2. The pH difference of each ratio is not significantly different, indicating that CO_2 can be equally dissolved in mixed electrolytes.

Table 6 Rate of CO$_2$ reduction products from ERC of each mixing ratio

Electrolyte	Mixing ratio	Rate of gaseous products (µmol/min)						Rate of liquid products (µmol/min)					
		CO	H$_2$	CH$_4$	C$_2$H$_4$	CO/H$_2$	CH$_4$/H$_2$	HCOO$^-$	Ethylene glycol	MeOH	EtOH	n-propanol	Acetone
KHCO$_3$:KCl	1:1	0.874	2.97	0.02	0	0.295	0.007	0.204	0.015	0.01	0.022	0	0.011
	1:2	1.251	4.85	0.12	0	0.257	0.025	0.240	0.012	0.01	0.016	0.022	0.013
	1:3	0.949	7.15	0.12	0	0.133	0.016	0.322	0.011	0	0.012	0.010	0.009
	1:4	0.308	2.83	0.05	0.004	0.110	0.017	0.440	0	0	0.045	0	0
CsHCO$_3$:CsCl	1:1	0.230	2.49	0	0	0.093	0	0.305	0	0	0	0	0
	1:2	0.142	1.06	0	0	0.134	0	0.342	0	0	0	0	0
	1:3	0.394	3.08	0.01	0	0.128	0.004	0.333	0	0	0.05	0	0
	1:4	0.292	4.47	0.01	0.008	0.065	0.002	0.248	0.031	0	0.06	0	0

For the mixed KHCO$_3$ with KCl, rate of CO decreased with increasing Cl$^-$ because CO is a key intermediate to reduce CO$_2$ into other products such as methane and ethylene [47]. Rate of CH$_4$ increased with increasing Cl$^-$ until the mixed ratio is 1:4, rate of CH$_4$ decrease and the formation of ethylene is originated. Due to an increasing Cl$^-$ concentration, the buffer capacity of electrolyte decreased, resulting in the higher local pH near electrode, which facilitates ethylene formation [48]. The formation of formate also increased with increasing Cl$^-$ due to the more reduction of HCO$_3^-$ as can be seen from Figure 30. Methanol and acetone production is not significantly different with increasing Cl$^-$. Ethanol, n-propanol and ethylene glycol decrease with increasing Cl$^-$. For KHCO$_3$+KCl with mixing ratio 1:4, ethanol production increased because the higher Cl$^-$, Cu-Cl catalytic layer could be generated. This catalytic layer facilitates more electron transfer to CO$_2$ [21].

For the mixed CsHCO$_3$ with CsCl, the formation of C$_2$ products such as ethylene and ethanol increased with increasing Cl$^-$ because Cl$^-$ ions can facilitate electron transfer to the unoccupied orbital of CO$_2$ [49]. Moreover, the more concentration of Cl$^-$ can result in formation of Cu-Cl catalytic layer that facilitate CO dimerization [50].

To deeply understand the effect of mixing ratio, LSV and EIS were used as the analytical techniques to discuss the experimental results.
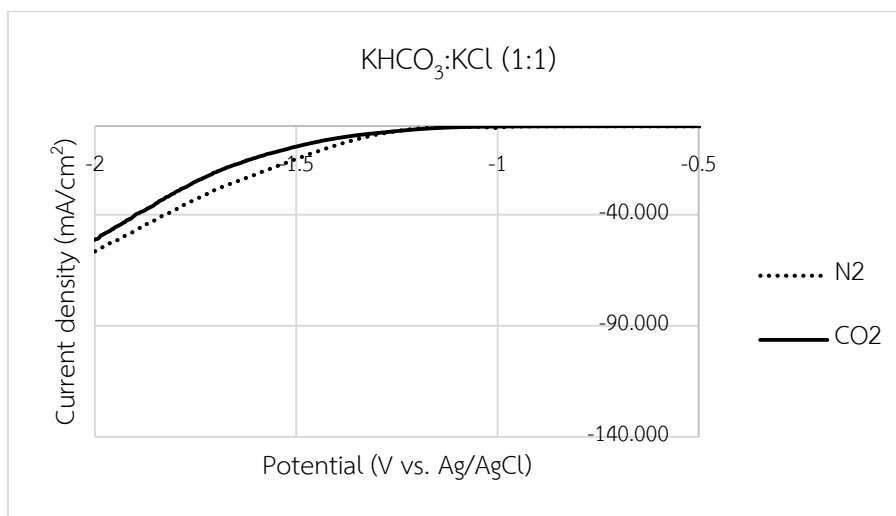
Figure 20 LSV of KHCO$_3$:KCl with mixing ratio 1:1

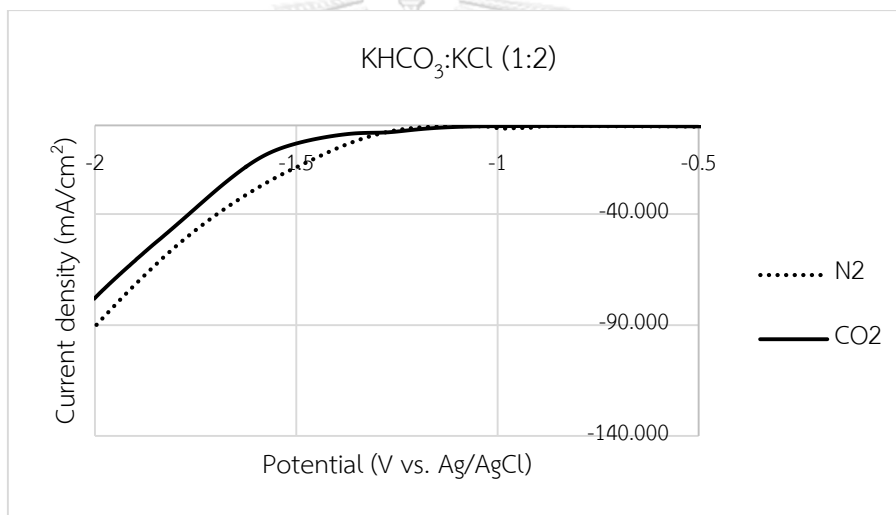*Figure 21 LSV of KHCO$_3$:KCl with mixing ratio 1:2*

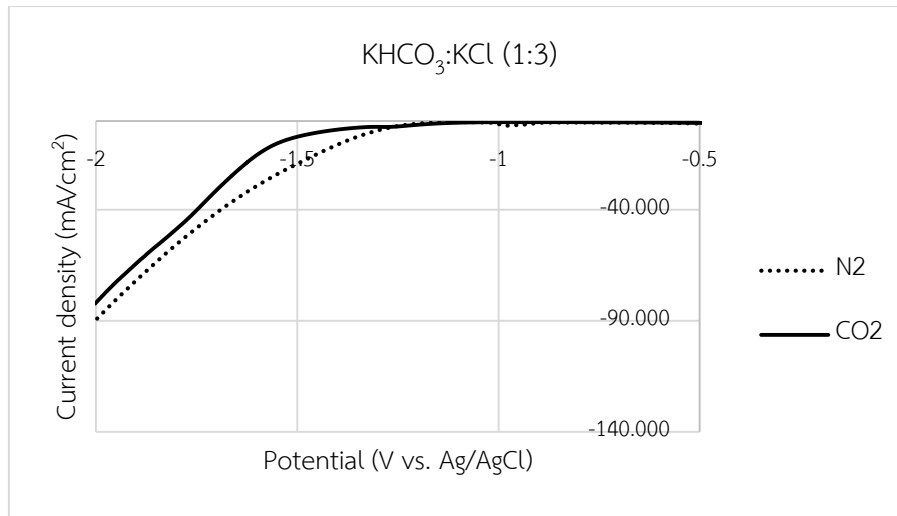*Figure 22 LSV of KHCO$_3$:KCl with mixing ratio 1:3*
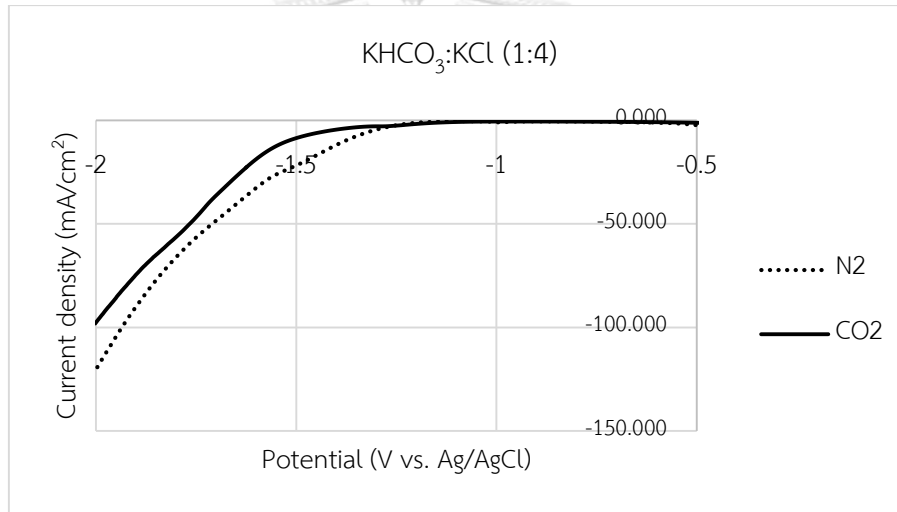
Figure 23 LSV of KHCO$_3$:KCl with mixing ratio 1:4

CsHCO$_3$:CsCl (1:1)

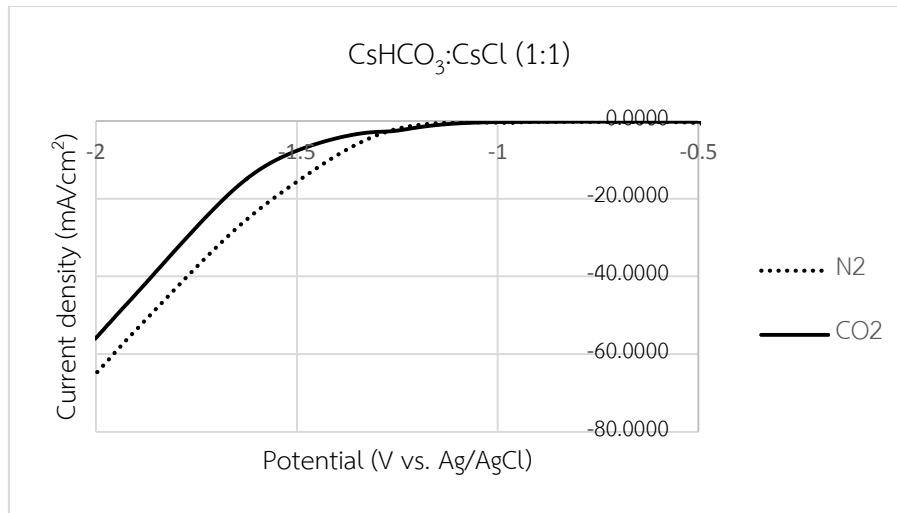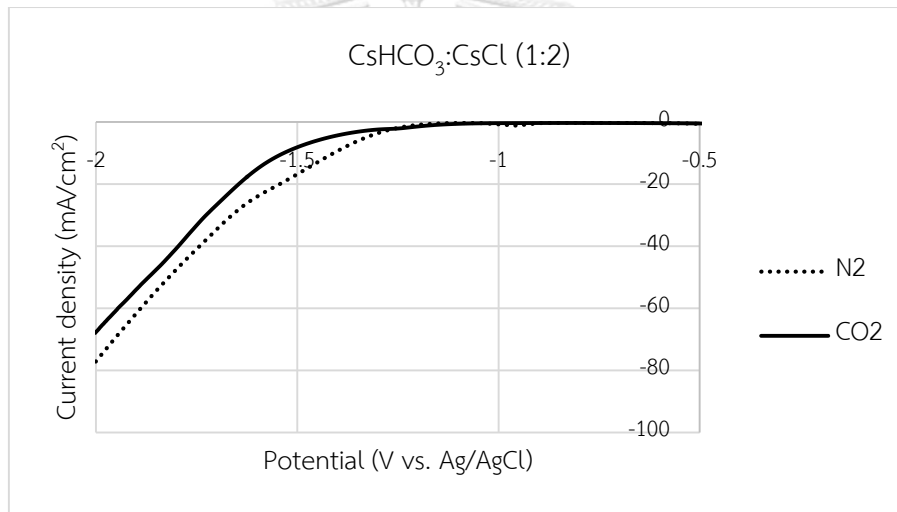*Figure 24 LSV of CsHCO$_3$:CsCl with mixing ratio 1:1*

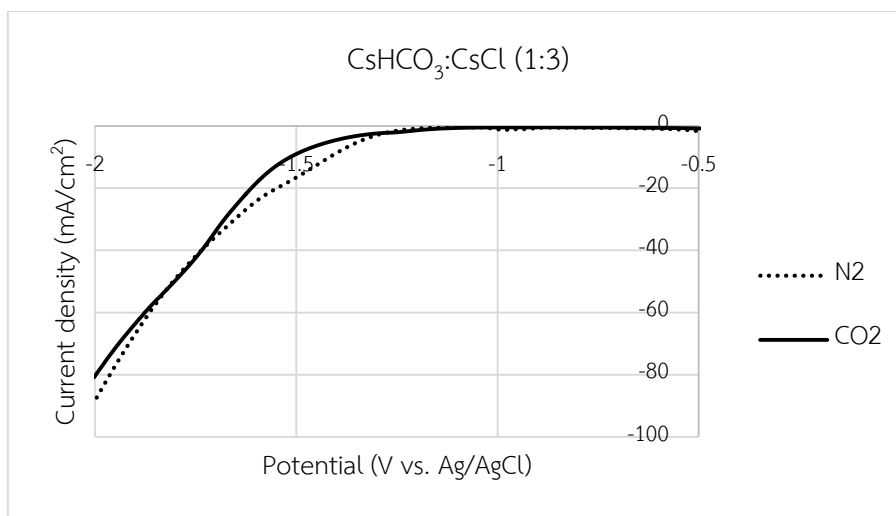CsHCO$_3$:CsCl (1:2)

Figure 25 LSV of CsHCO$_3$:CsCl with mixing ratio 1:2

Figure 26 LSV of CsHCO$_3$:CsCl with mixing ratio 1:3
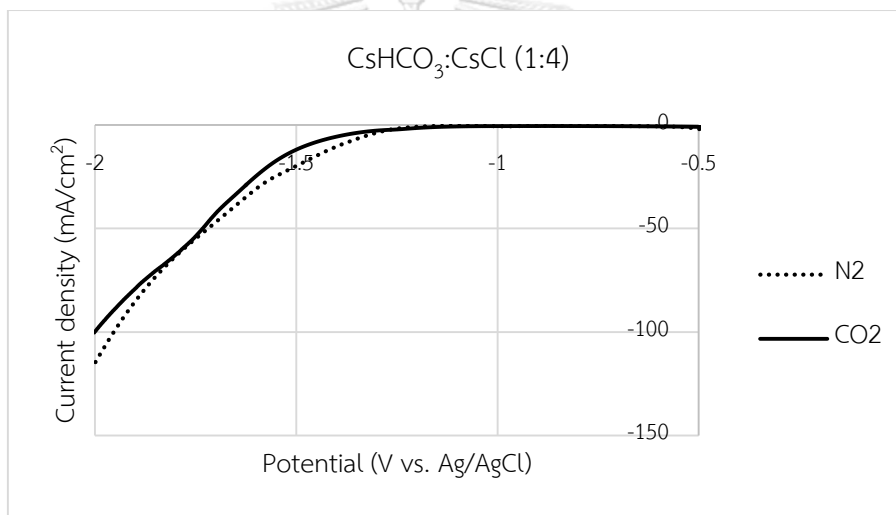
Figure 27 LSV of CsHCO$_3$:CsCl with mixing ratio 1:4

Figure 20-27 shows the LSV of mixed electrolyte for K^+ cation (Figure 20-23) and Cs^+ cation (24-27) with various ratios. Under CO_2 saturated conditions, solid line represents the ERC and HER. In the presence of N_2, which presented in dash line represents the HER. When the potential becomes more negative, hydronium ions (H_3O^+) are oriented with hydrogen side toward the electrode surface. As increasing more negative potential, adsorbed hydrogen is formed from these hydronium ions, and finally, H_2 is produced, resulting in the dramatically increasing of current density.
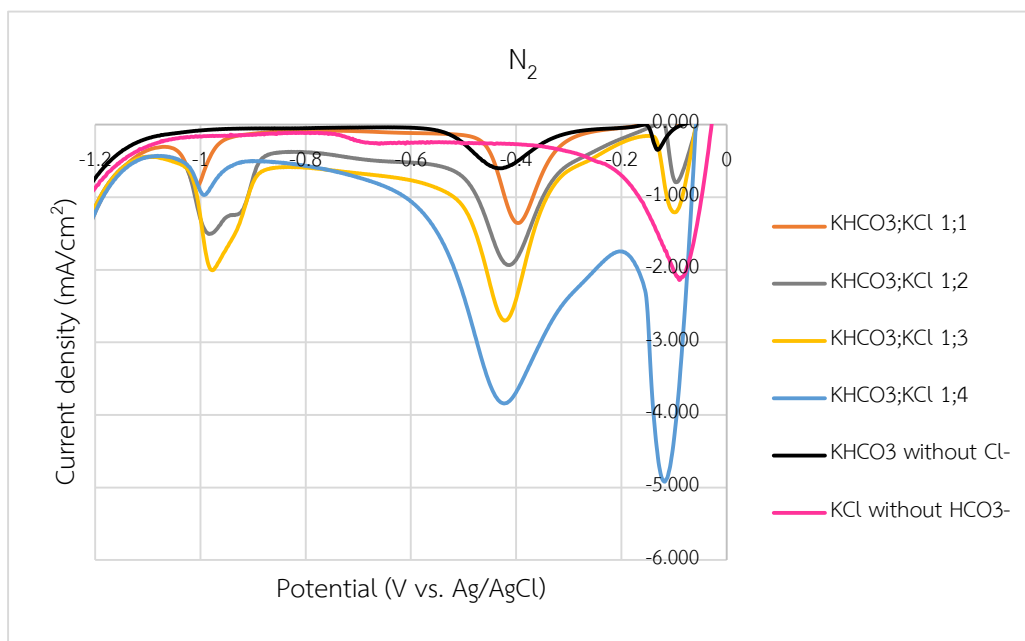
Figure 28 LSV of KHCO₃:KCl with various ratio compared with single electrolyte under
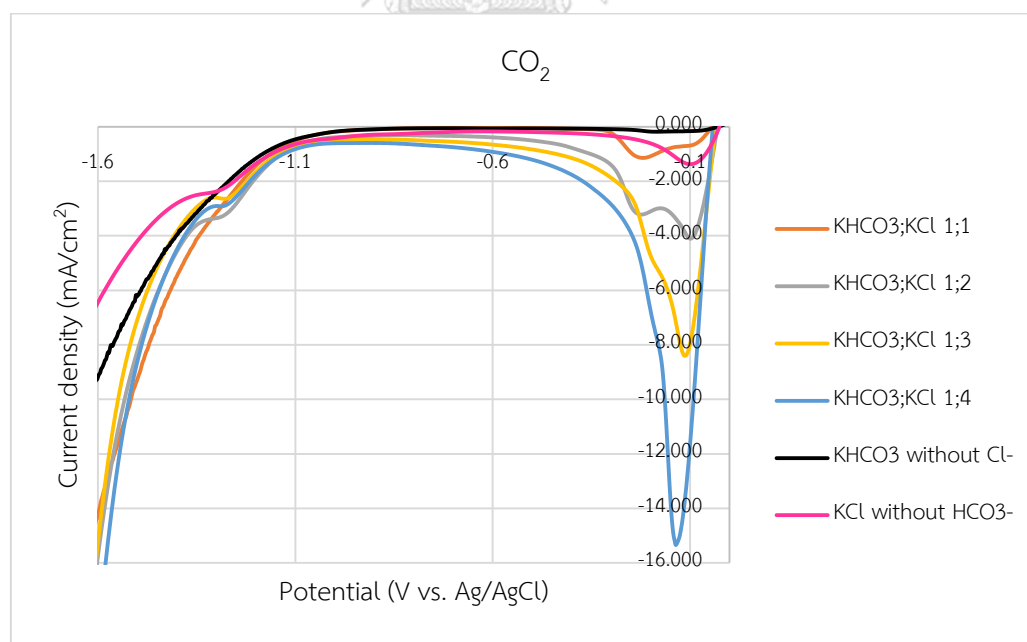
N₂ saturation

Figure 29 LSV of KHCO₃:KCl with various ratio compared with single electrolyte under
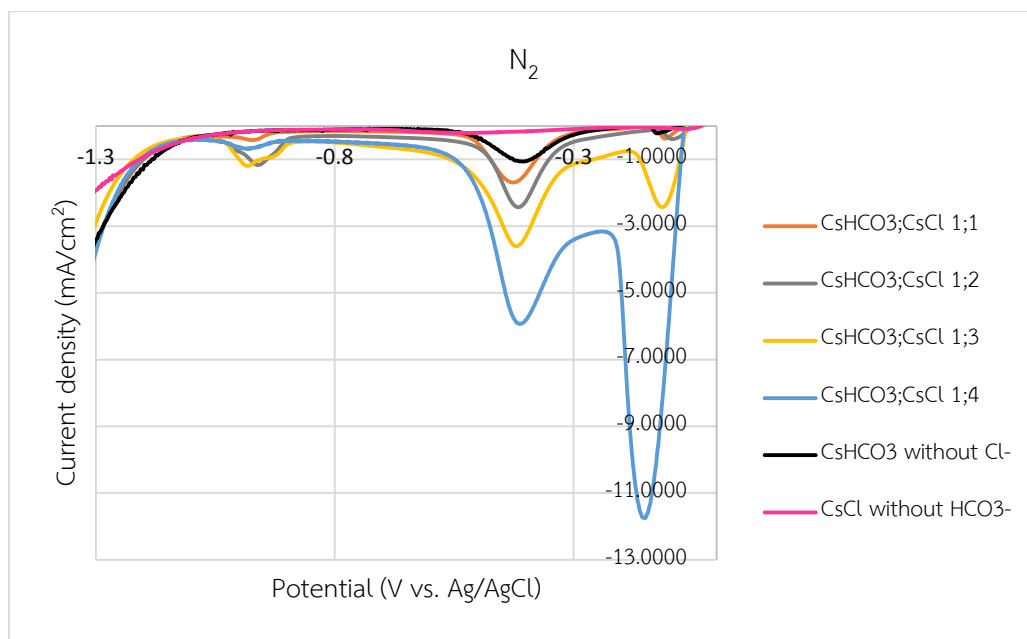
CO₂ saturation

Figure 30 LSV of CsHCO₃:CsCl with various ratio compared with single electrolyte under N₂ saturation

Figure 31 LSV of CsHCO₃:CsCl with various ratio compared with single electrolyte under CO₂ saturation

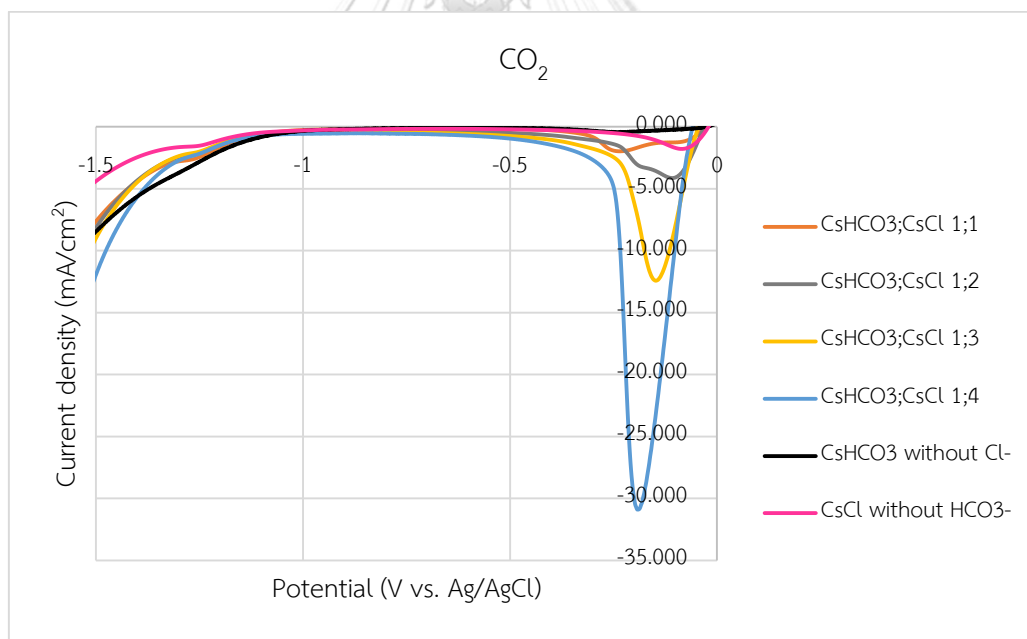Figure 28-31 shows the LSV of mixed electrolytes with various HCO_3^-:Cl^- ratios including K^+ cation (Figure 28,29) and Cs^+ cation (Figure 30,31) compared with single electrolytes. Under N_2 saturation (Figure 28 and 30), the mixed electrolyte exhibited

three reduction peaks. The first peak corresponded to the reduction of the CuO to Cu [42]. The second reduction peak is detected around -0.4V vs. Ag/AgCl, this peak attributed to the direct reduction of HCO_3^- to formate [45] because it cannot be seen in the absence of HCO_3^- electrolyte. The last reduction peak, located around -1.0V vs. Ag/AgCl, this reduction peak can be arisen from the proton reduction. For single reduction (figure 18a and 19a), the proton reduction peak located at -0.5V vs. Ag/AgCl but in mixed electrolyte proton reduction peak was shifted to -1.0V vs. Ag/AgCl, which may be due to the strongly adsorption of Cl^-. $KHCO_3$:KCl with 1:3 mixing ratio exhibits the highest proton reduction current density, indicating the fastest electron transfer, resulting in the highest H_2 production. For CO_2 saturation as shown in Figure 29 and 31, there are small reduction peaks when using single electrolyte. For mixed electrolyte, the bigger reduction peak can be observed. The first reduction peak can be attributed to the reduction of HCO_3^- to formate, the formation of adsorbed CO [45] and the reduction of CuO to Cu [42] because of the higher current density compared with N_2 saturated conditions. As can be seen from Table 6, ethanol and n-propanol decreased with increasing Cl^- until the ratio is 1:3. It was found that ethanol and n-propanol production can be facilitated by CuO [51]. The more Cl^-, the more CuO was reduced, can be seen from a higher current density. The decreasing of CuO resulting in the decreased in n-propanol and ethylene glycol, which is the intermediate to ethanol formation. The more Cl^- concentration, the Cu-Cl catalytic layer could be easily formed. This catalytic layer facilitates the electron transfer and restrains the CO_2, resulting in the higher CO_2 reduction current [21]. The higher CO_2 reduction current density indicates that there could be more adsorbed CO and increases the possibility to reduce CO_2 to C_2 product such as ethylene and ethanol via CO dimerization. There is a small reduction peak around -1.3V vs. Ag/AgCl that presence only with Cl^- anions, this could be attributed to the reduction of chloride because it cannot be seen in the single HCO_3^- containing electrolyte.
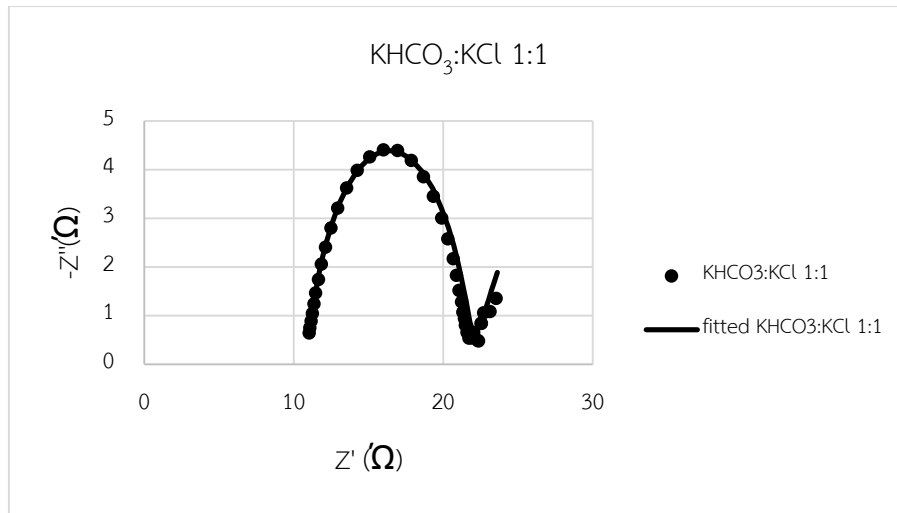
Figure 32 Nyquist plot of KHCO₃:KCl (1:1) under CO₂ saturation

Figure 33 Nyquist plot of KHCO₃:KCl (1:2) under CO₂ saturation

Figure 34 Nyquist plot of KHCO$_3$:KCl (1:3) under CO$_2$ saturation
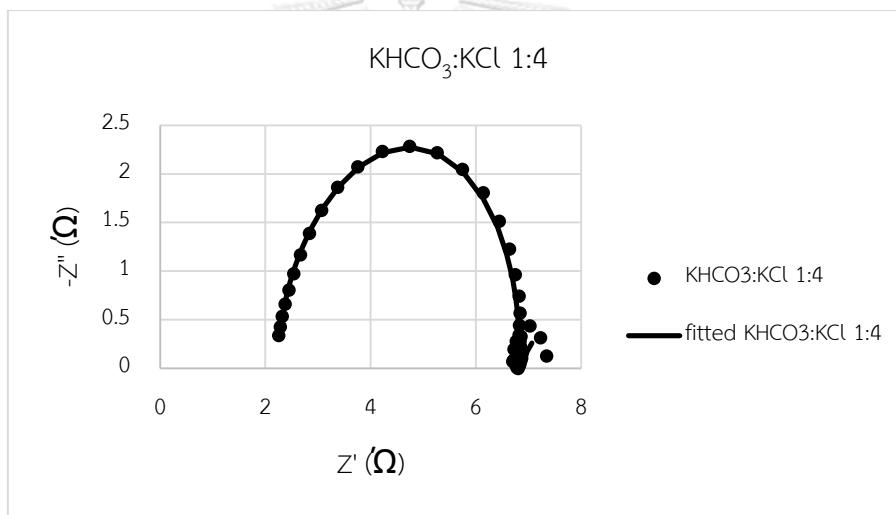
Figure 35 Nyquist plot of KHCO$_3$:KCl (1:4) under CO$_2$ saturation
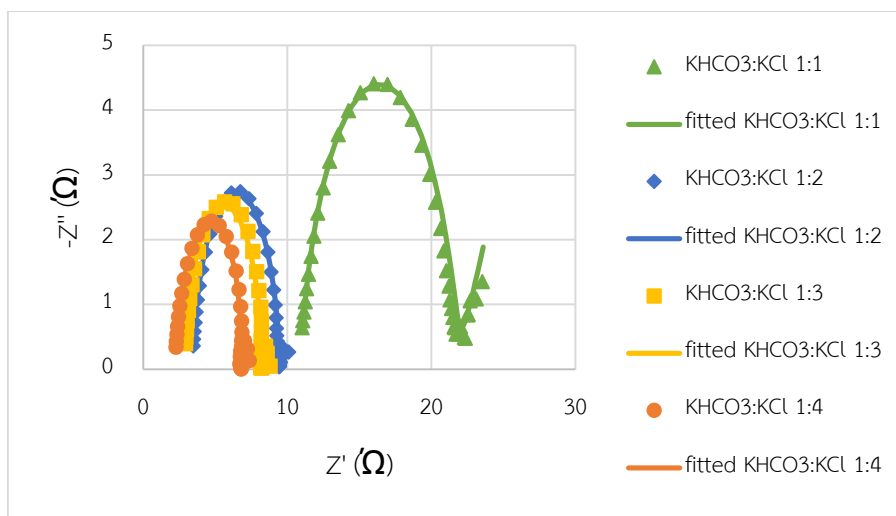
Figure 36 Nyquist plot of KHCO$_3$:KCl with several ratios under CO$_2$ saturation

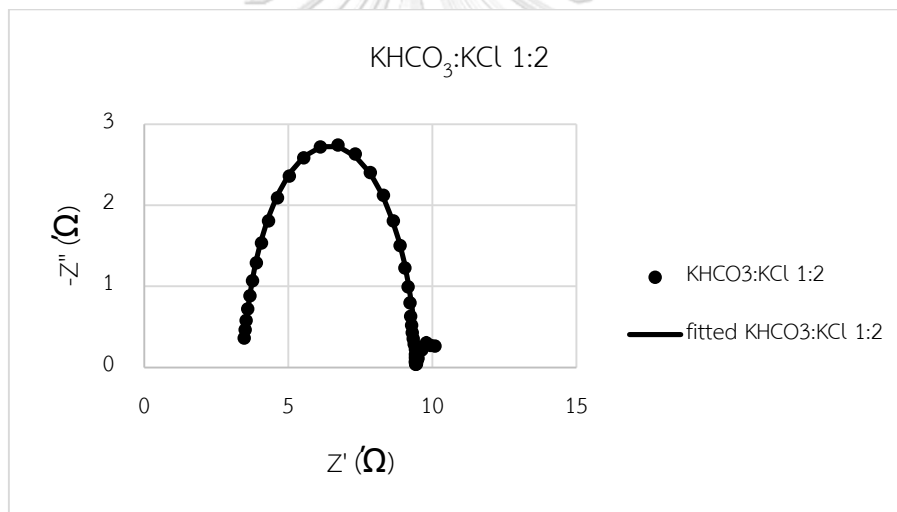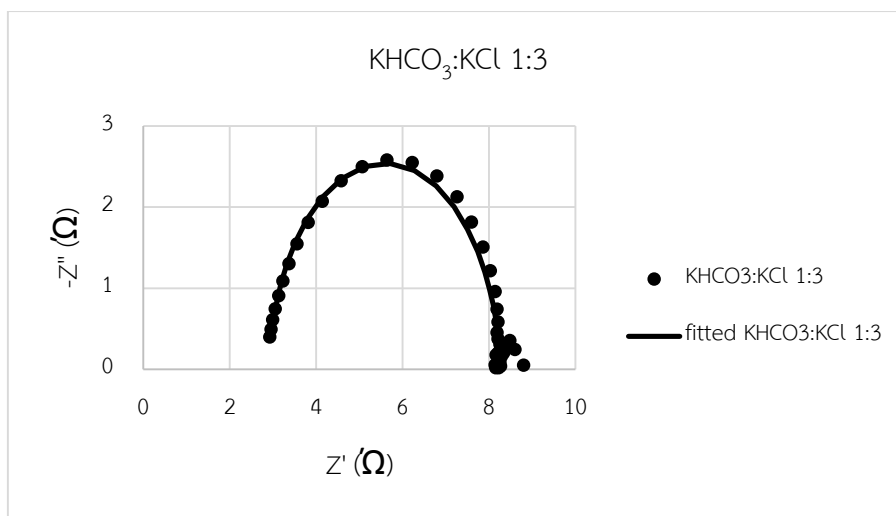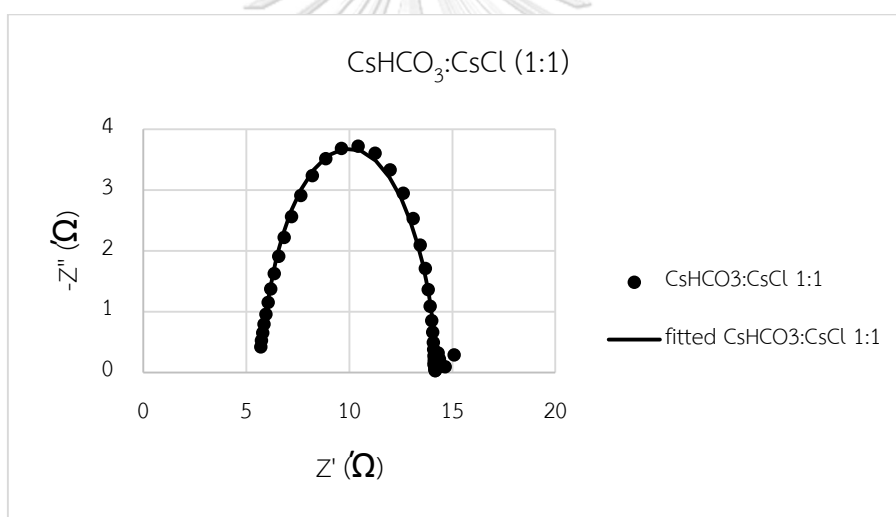*Figure 37 Nyquist plot of CsHCO$_3$:CsCl (1:1) under CO$_2$ saturation*
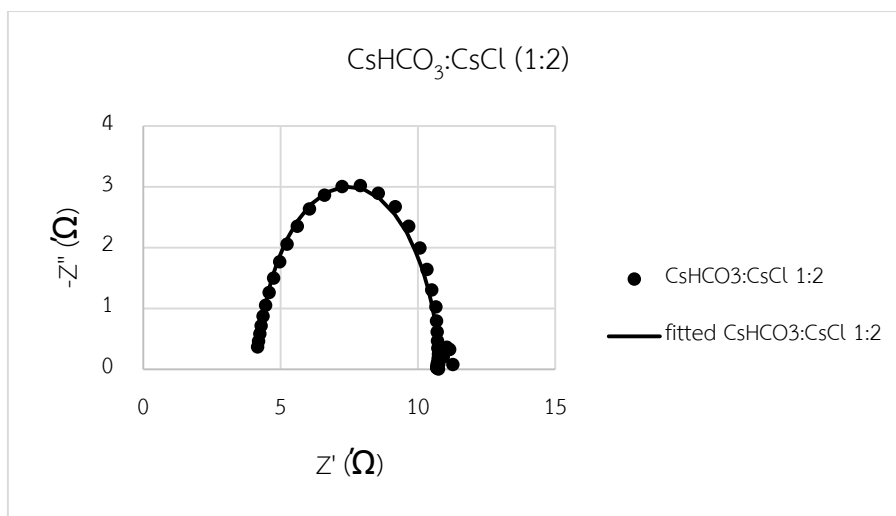
Figure 38 Nyquist plot of CsHCO₃:CsCl (1:2) under CO₂ saturation
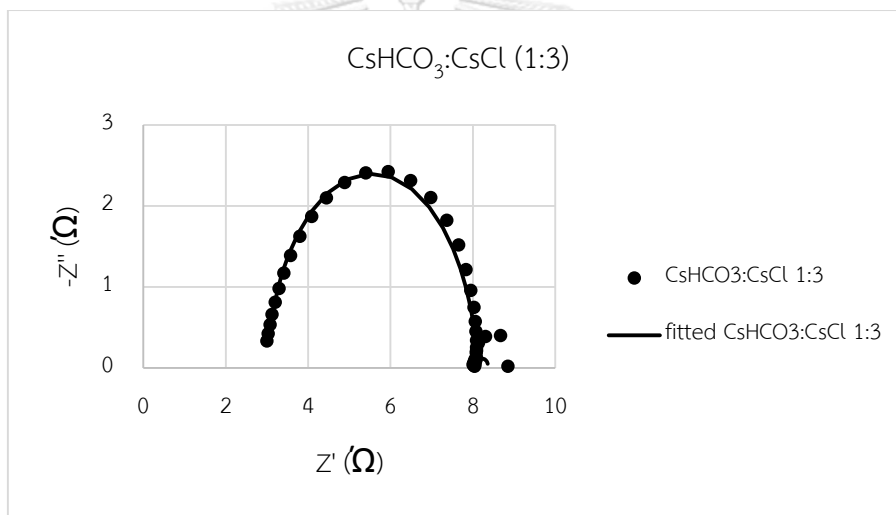
Figure 39 Nyquist plot of CsHCO₃:CsCl (1:3) under CO₂ saturation
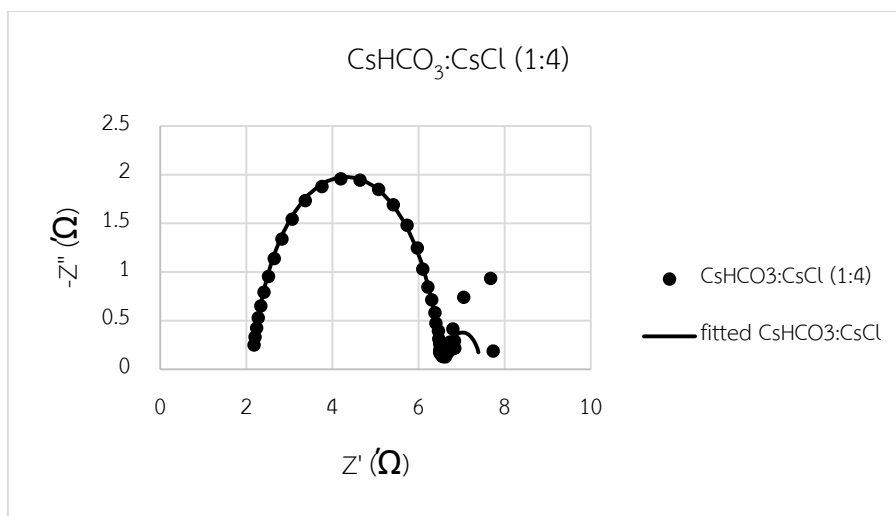
Figure 40 Nyquist plot of CsHCO$_3$:CsCl (1:4) under CO$_2$ saturation
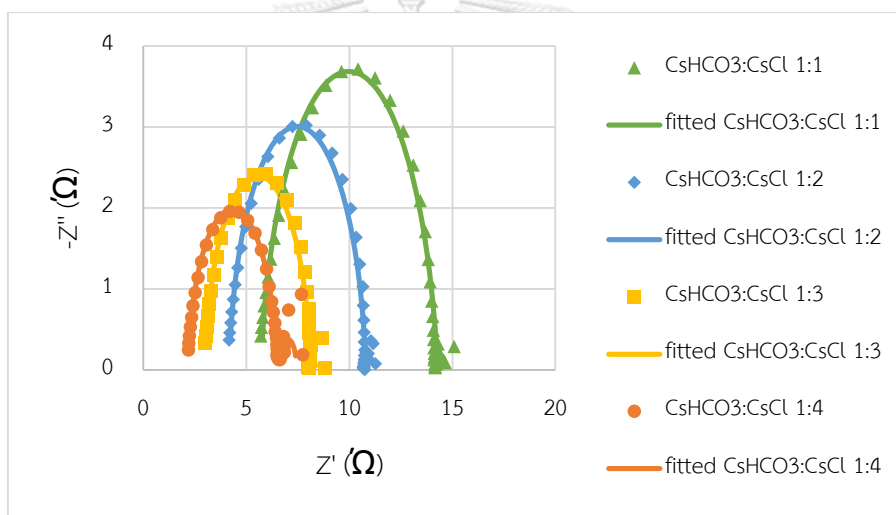
Figure 41 Nyquist plot of KHCO$_3$:KCl with several ratios under CO$_2$ saturation

From Figure 36 and 41, the first value of the semi-circle represents the resistance of solution (R$_s$). R$_s$ of each mixing ratio is different due to the difference in the amount of Cl$^-$ ions. The value of R$_s$ from table 7 decreased with increasing Cl-, suggesting that the conductivity of mixed electrolyte increased with increasing Cl$^-$. The higher conductivity of mixed electrolyte, the lesser polarization loss. The decreasing of polarization loss can drive the kinetics overpotentials, resulting in CO$_2$ can be further reduced to C2+ products. The semi-circle in high frequencies range indicates the electron transfer process and the diameter of the semi-circle is equal to the resistance of charge transfer (R$_{ct}$) [25]. The bigger diameter, indicating the higher R$_{ct}$. There are two semi-circle for mixed electrolyte with increasing Cl$^-$ in the low

frequencies range. The small semi-circle could be attributed to the presence of Cu-Cl catalytic film layer that facilitates the electron transfer from the electrode to CO_2 [21]. Because the Cu-Cl catalytic layer facilitates the electron transfer, resulting in the easier reduction of CO_2 into many products. Furthermore, as can be seen from Table 7 the value of R_{ct} decreased with increasing Cl^-, demonstrating that the intermediates in electrolytes diffuse more easily [52].

To obtain the value of solution resistance (R_s) and charge transfer resistance (R_{ct}), the electrochemical circuit fit has to be carried out as shown in figure 42.
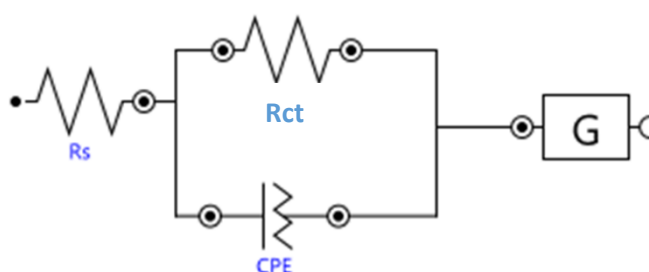
Figure 42 Circuit fitted from EIS

The circuit was composed of R_s, R_{ct}, Constant phase element (CPE), and Gerischer impedance (G). CPE represents the non-ideal capacitors, that difference from the ideal capacitor behavior. For an ideal capacitor, the electrode surface was assumed to be uniformly smooth [53]. However, as can be seen from figure 8 the surface of copper electrode is rough, the CPE was used in the circuit. Gerischer impedance (G) was fitted to the experiment data due to the presence of Cu-Cl catalytic layer that can facilitate electron transfer. Gerischer impedance indicates a faster charge transfer process followed by a mass transfer process for CO_2 electrochemical reduction reaction, including dissociative adsorption and the subsequent surface diffusion of the reaction intermediate species [54].

Table 7 Calculated R_s and R_{ct} from circuit fitting

Electrolyte	Mixing ratio	R_s (Ω)	R_{ct} (Ω)	Fitting error (χ^2)
KHCO$_3$:KCl	1:1	11.00	10.56	0.013
	1:2	3.47	5.96	0.012
	1:3	2.97	5.33	0.015
	1:4	2.25	4.87	0.019
CsHCO$_3$:CsCl	1:1	5.70	8.52	0.011
	1:2	4.16	6.59	0.014
	1:3	3.01	5.07	0.035
	1:4	2.18	4.22	0.080

4.2.3 Part III Effect of applied potential

Although methane and ethylene are the major hydrocarbon products from ERC over Cu electrode, CH$_4$ is easier to be produced due to the less number of electron transfer. KHCO$_3$+KCl with mixing ratio 1:2 was chosen to investigate the effect of applied potential because it produce the highest CH$_4$/H$_2$ ratio.

Table 8 CO$_2$ products formation rate with various applied potentials

Potential (V vs. Ag/AgCl)	Rate of gaseous product (µmol/min)						Rate of liquid product (µmol/min)					
	CO	CH$_4$	H$_2$	C$_2$H$_4$	CO/H$_2$	CH$_4$/H$_2$	HCOO$^-$	Ethylene glycol	Acetone	MeOH	EtOH	n-Propanol
-1.2	0	0	0.45	0	0	0	0	0	0	0	0	0
-1.4	0.05	0	1.55	0	0.029	0	0.07	0	0	0	0	0
-1.6	1.25	0.12	4.85	0	0.257	0.025	0.240	0.012	0.013	0.010	0.016	0.02
-1.8	0.41	1.03	18.94	0	0.021	0.054	0.43	0	0	0	0.043	0.07
-2.0	0.47	1.00	21.84	0.005	0.021	0.046	0.42	0	0	0	0.068	0.05

Table 8 shows the rate of CO_2 reduction products with various applied potentials. At -1.2V vs. Ag/AgCl, no CO_2 reduction products were observed, demonstrating that CO_2 reduction did not occur. For -1.4V vs. Ag/AgCl, CO and formate were observed due to the requirement of only two electron transfer [10]. As the applied potentials become more negative, surface bound C1 specie, CO is more likely to be further reduced to methane and desorb [38], resulting in the increasing of methane and decreasing of CO production. At very negative potentials, the C_2 hydrocarbon product, ethylene and the higher alcohol such as ethanol and n-propanol increased because of the dimerization of CO yielded ethylene and other C2+ products at high potentials [48]. Furthermore, HER increased with increasing the applied potentials because of the mass transfer limit of CO_2, which take place at the current density from CO_2 electrolysis is over 20mA/cm^2 [8]. As can be seen from Figure 43, the current density at the applied potential is more negative than -1.8V vs. Ag/AgCl was exceeded 20 mA/cm^2. Proton and electron transfer faster while CO_2 transfers with the same rate due to the mass transfer limit, resulting in the dramatically increase H_2 formation.
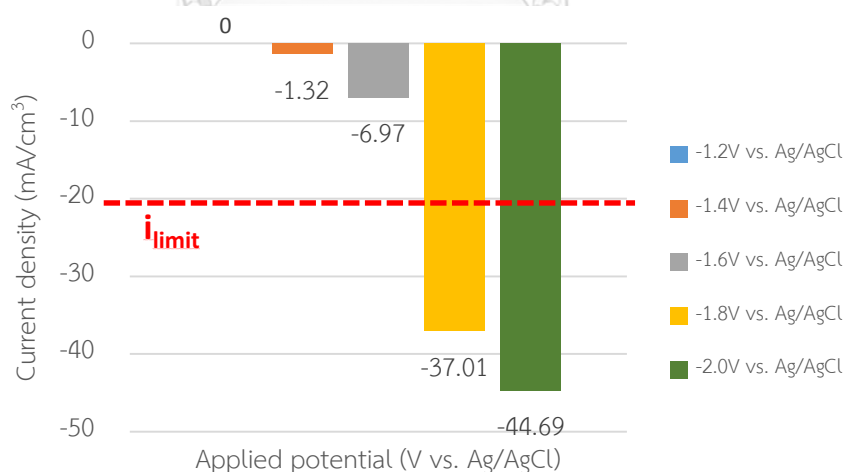

Figure 43 Current density from CO$_2$ electrolysis at various applied potentials

Chapter V

Conclusions and Recommendation

5.1 Conclusions

For the effect of anions when Cs^+ cation was fixed, Cl^- exhibited the highest CO/H_2 production because the strongly adsorption of Cl^- on the electrode surface not only facilitated electron transfer to CO_2 but also blocked the sites for HER simultaneously. SO_4^{2-} exhibited the highest H_2 formation due to the fastest proton reduction as can be seen from LSV results. Moreover, electrolyte containing SO_4^{2-} is acidic solution, which promotes H_2 evolution. However, it is the only anion that can produce ethylene glycol due to the acidic conditions favor the production of glyoxal, the intermediate to ethylene glycol. $CsHCO_3$ generated the highest formate because the HCO_3^- can be directly reduced to formate. For the effect of cations when Cl^- was fixed as anion. The CO/H_2 production increased with increasing cation size in the order: $Na^+ < K^+ < Cs^+$ because of the higher formation rate of adsorbed CO and slower proton reduction as confirmed by the LSV results.

Mixing of HCO_3^- and Cl^- can improve the performance of electrolyte because of the decreasing of polarization loss. According to the LSV and EIS results, the improved performance of electrolyte with increasing Cl^- correlated well with the presence of Cu-Cl catalytic layer that can facilitate electron transfer integrated with the easier diffusion of intermediate species.

Besides the effect of electrolyte, the effect of applied potentials was further studied. At low negative potentials, CO and formate were observed as CO_2 reduction products due to the low energy barrier, requires only two electron transfer. As the potentials is more negative not only CO intermediate species is further reduced to other CO_2 reduction products such as methane, ethylene and ethanol but HER is also increased because of the mass transfer limit of CO_2.

5.2 Recommendations

The study of another solution in the ERC that can suppress HER, the competitive reaction such as ionic liquid or non-aqueous electrolyte.

REFERENCES

1. Lu, Q. and F. Jiao, *Electrochemical CO2 reduction: Electrocatalyst, reaction mechanism, and process engineering.* Nano Energy, 2016. **29**: p. 439-456.

2. Uemoto, N., et al., *Electrochemical Carbon Dioxide Reduction in Methanol at Cu and Cu2O-Deposited Carbon Black Electrodes.* ChemEngineering, 2019. **3**(1).

3. Konig, M., et al., *Solvents and Supporting Electrolytes in the Electrocatalytic Reduction of CO2.* iScience, 2019. **19**: p. 135-160.

4. Kuhl, K.P., et al., *Electrocatalytic conversion of carbon dioxide to methane and methanol on transition metal surfaces.* J Am Chem Soc, 2014. **136**(40): p. 14107-13.

5. Allen J. Bard, L.R., *Electrochemical Methods Fundamentals and Applications*. 2 ed. Introduction and Overview of Electrode process, ed. E.S. David Harris, Charity Robey, Eugene Aiello. 2001, United state of America: John Wiley & Sons, Inc.

6. Dixit, R.J. and C.B. Majumder, *CO2 capture and electro-conversion into valuable organic products: A batch and continuous study.* Journal of CO2 Utilization, 2018. **26**: p. 80-92.

7. Wang, W.-N., et al., *Comparison of CO2 Photoreduction Systems: A Review.* Aerosol and Air Quality Research, 2014. **14**(2): p. 533-549.

8. Sun, D. and Y. Chen, *Electrode Kinetics of CO2 Electroreduction*, in *Electrochemical Reduction of Carbon Dioxide*. 2016. p. 103-154.

9. Chen, C., J.F. Khosrowabadi Kotyk, and S.W. Sheehan, *Progress toward Commercial Application of Electrochemical Carbon Dioxide Reduction.* Chem, 2018. **4**(11): p. 2571-2586.

10. Garg, S., et al., *Advances and challenges in electrochemical CO2 reduction processes: an engineering and design perspective looking beyond new catalyst materials.* Journal of Materials Chemistry A, 2020. **8**(4): p. 1511-1544.

11. Nitopi, S., et al., *Progress and Perspectives of Electrochemical CO2 Reduction on Copper in Aqueous Electrolyte.* Chem Rev, 2019.

12. Wang, Y., C. Niu, and D. Wang, *Metallic nanocatalysts for electrochemical CO2*

reduction in aqueous solutions. J Colloid Interface Sci, 2018. **527**: p. 95-106.

13. Hori, Y., *Electrochemical CO2 Reduction on Metal Electrodes*, ed. C. Vayenas et al. Vol. 42. 2008, New York: Springer.

14. Vasileff, A., et al., *Surface and Interface Engineering in Copper-Based Bimetallic Materials for Selective CO2 Electroreduction.* Chem, 2018. **4**(8): p. 1809-1831.

15. Ren, D., J. Fong, and B.S. Yeo, *The effects of currents and potentials on the selectivities of copper toward carbon dioxide electroreduction.* Nat Commun, 2018. **9**(1): p. 925.

16. J. Albo, M.l.-G., P. Castaño, A. Irabien, *Towards the electrochemical conversion of carbon dioxide into methanol.* Green Chemistry, 2012. **0**: p. 1-3.

17. Akira Murata, Y.H., *Product Selectivity Affected by Cationics Species in Electrochemical Reduction of CO2 and CO at a Cu Electrode.* The Chemical Society of Japan, 1991. **64**: p. 123-127.

18. Wu, J., et al., *Electrochemical Reduction of Carbon Dioxide I. Effects of the Electrolyte on the Selectivity and Activity with Sn Electrode.* Journal of The Electrochemical Society, 2012. **159**(7): p. F353-F359.

19. Singh, M.R., et al., *Hydrolysis of Electrolyte Cations Enhances the Electrochemical Reduction of CO2 over Ag and Cu.* J Am Chem Soc, 2016. **138**(39): p. 13006-13012.

20. Lum, Y., et al., *Optimizing C–C Coupling on Oxide-Derived Copper Catalysts for Electrochemical CO2 Reduction.* The Journal of Physical Chemistry C, 2017. **121**(26): p. 14191-14203.

21. Ogura, K., et al., *CO2 attraction by specifically adsorbed anions and subsequent accelerated electrochemical reduction.* Electrochimica Acta, 2010. **56**(1): p. 381-386.

22. Huang, Y., C.W. Ong, and B.S. Yeo, *Effects of Electrolyte Anions on the Reduction of Carbon Dioxide to Ethylene and Ethanol on Copper (100) and (111) Surfaces.* ChemSusChem, 2018. **11**(18): p. 3299-3306.

23. Nguyen, D.L.T., et al., *Effect of halides on nanoporous Zn-based catalysts for highly efficient electroreduction of CO 2 to CO.* Catalysis Communications, 2018. **114**: p. 109-113.

24.   Varela, A.S., et al., *Tuning the Catalytic Activity and Selectivity of Cu for CO2 Electroreduction in the Presence of Halides.* ACS Catalysis, 2016. **6**(4): p. 2136-2144.

25.   Hong, S., et al., *Anion dependent CO/H 2 production ratio from CO 2 reduction on Au electro-catalyst.* Catalysis Today, 2017. **295**: p. 82-88.

26.   Paschkewitz, T. *Linear Sweep Voltammetry (LSV).* 2020; Available from: https://pineresearch.com/shop/kb/software/methods-and-techniques/voltammetric-methods/linear-sweep-voltammetry-lsv/.

27.   Department of Chemical Engineering and Biotechnology, U.o.C. *Linear Sweep and Cyclic Voltametry: The Principles.* Available from: https://www.ceb.cam.ac.uk/research/groups/rg-eme/Edu/linear-sweep-and-cyclic-voltametry-the-principles.

28.   Bontempelli, G., N. Dossi, and R. Toniolo, *Linear Sweep and Cyclic ✰*, in *Reference Module in Chemistry, Molecular Sciences and Chemical Engineering*. 2016.

29.   P, W., *Electrochemical Impedance Spectroscopic Study of Polyaniline Sensor for Contactless Conductivity Measurement* 2013, Rajamangala University of Technology Krungthep.

30.   Lim, C.F.C., *ELECTROCHEMICAL REDUCTION OF CARBON DIOXIDE ON COPPER ELECTRODES*. 2017, University of Canterbury: Chemical and Process Engineering.

31.   P, K., *Testing of Membrane Electrode Assembly Performance by Electrochemical Impedance Spectroscopy*, in *Department of Chemical Technology*. 2005, Chulalongkorn University.

32.   A, S. *Electrochemical arsenic remediation for rural Bangladesh*. 2008; Available from: https://www.researchgate.net/publication/241588665_Electrochemical_arsenic_remediation_for_rural_Bangladesh.

33.   Ming Ma, S.K., Ib Chorkendorff and Brian Seger, *Role of Ion-Selective Membranes in the Carbon Balance for CO2 Electroreduction via Gas Diffusion Electrode Reactor Designs*, T.U.o. Denmark, Editor. 2020.

34. *Proton Conducting Membrane Fuel Cell IV*, K.O. M. Murthy, J.W. Van Zee, S.R. Narayanan, E.S. Takeuchi, Editor. 2006, The Electrochemical Society, Inc.: USA.

35. Choi, J., et al., *Electrochemical CO 2 reduction to CO on dendritic Ag–Cu electrocatalysts prepared by electrodeposition.* Chemical Engineering Journal, 2016. **299**: p. 37-44.

36. Haynes, W.M., *CRC Handbook of Chemistry and Physics*. 2013-2014, Boca Raton: FL.

37. Zhong, H., K. Fujii, and Y. Nakano, *Effect of KHCO3Concentration on Electrochemical Reduction of CO2on Copper Electrode.* Journal of The Electrochemical Society, 2017. **164**(9): p. F923-F927.

38. Kuhl, K.P., et al., *New insights into the electrochemical reduction of carbon dioxide on metallic copper surfaces.* Energy & Environmental Science, 2012. **5**(5).

39. Schmid, B., et al., *Reactivity of Copper Electrodes towards Functional Groups and Small Molecules in the Context of CO2 Electro-Reductions.* Catalysts, 2017. **7**(5).

40. Gao, D., F. Scholten, and B. Roldan Cuenya, *Improved CO2 Electroreduction Performance on Plasma-Activated Cu Catalysts via Electrolyte Design: Halide Effect.* ACS Catalysis, 2017. **7**(8): p. 5112-5120.

41. Varela, A.S., et al., *Controlling the selectivity of CO2 electroreduction on copper: The effect of the electrolyte concentration and the importance of the local pH.* Catalysis Today, 2016. **260**: p. 8-13.

42. Giri, S.D. and A. Sarkar, *Electrochemical Study of Bulk and Monolayer Copper in Alkaline Solution.* Journal of The Electrochemical Society, 2016. **163**(3): p. H252-H259.

43. Kortlever, R., et al., *Electrochemical carbon dioxide and bicarbonate reduction on copper in weakly alkaline media.* Journal of Solid State Electrochemistry, 2013. **17**(7): p. 1843-1849.

44. Soliman, A.B., et al., *The potential of a graphene-supported porous-organic polymer (POP) for CO2 electrocatalytic reduction.* Chem Commun (Camb), 2016. **52**(81): p. 12032-12035.

45. Chen, C.S., et al., *Stable and selective electrochemical reduction of carbon dioxide to ethylene on copper mesocrystals.* Catalysis Science & Technology, 2015. **5**(1): p. 161-168.

46. Waegele, M.M., et al., *How cations affect the electric double layer and the rates and selectivity of electrocatalytic processes.* J Chem Phys, 2019. **151**(16): p. 160902.

47. Nie, X., et al., *Reaction mechanisms of CO2 electrochemical reduction on Cu(111) determined with density functional theory.* Journal of Catalysis, 2014. **312**: p. 108-122.

48. Kortlever, R., et al., *Catalysts and Reaction Pathways for the Electrochemical Reduction of Carbon Dioxide.* J Phys Chem Lett, 2015. **6**(20): p. 4073-82.

49. Fu, H.Q., et al., *Enhanced CO2 electroreduction performance over Cl-modified metal catalysts.* Journal of Materials Chemistry A, 2019. **7**(20): p. 12420-12425.

50. Eilert, A., et al., *Formation of Copper Catalysts for CO2 Reduction with High Ethylene/Methane Product Ratio Investigated with In Situ X-ray Absorption Spectroscopy.* J Phys Chem Lett, 2016. **7**(8): p. 1466-70.

51. Rahaman, M., et al., *Electrochemical Reduction of CO2 into Multicarbon Alcohols on Activated Cu Mesh Catalysts: An Identical Location (IL) Study.* ACS Catalysis, 2017. **7**(11): p. 7946-7956.

52. Yang, D.-w., et al., *Electrochemical Impedance Studies of CO 2 Reduction in Ionic Liquid/Organic Solvent Electrolyte on Au Electrode.* Electrochimica Acta, 2016. **189**: p. 32-37.

53. Sun, J. and Y. Liu, *Unique Constant Phase Element Behavior of the Electrolyte-Graphene Interface.* Nanomaterials (Basel), 2019. **9**(7).

54. Irvine, X.Y.a.J.T.S., *Understanding of CO2 Electrochemical Reduction Reaction Process via High Temperature Solid Oxide Electrolysers.* The Electrochemical Society, 2015. **68**: p. 3535-3551.

VITA

NAME	Siraphat Somchit
DATE OF BIRTH	30 December 1995
PLACE OF BIRTH	Bangkok, Thailand
INSTITUTIONS ATTENDED	B.Eng Chemical Engineering Faculty of Engineering, Thammasat University
HOME ADDRESS	59/11-12 Prachatippatai Road, Thapileang Subdistrict, Muang District, Suphanburi Province 72000

จุฬาลงกรณ์มหาวิทยาลัย
CHULALONGKORN UNIVERSITY